Synthetic talc and talc-like structures: preparation, features and applications

Marie Claverie, Angela Dumas, Christel Careme, Mathilde Poirier, Christophe Le roux, Pierre Micoud, François Martin, Cyril Aymonier

Synthetic talc and talc-like structures: preparation, features and applications.

Marie Claverie,[a] Angela Dumas,[b] Christel Careme,[a] Mathilde Poirier,[b] Christophe Le Roux,[b] Pierre Micoud,[b] François Martin,*[b] and Cyril Aymonier *[c]

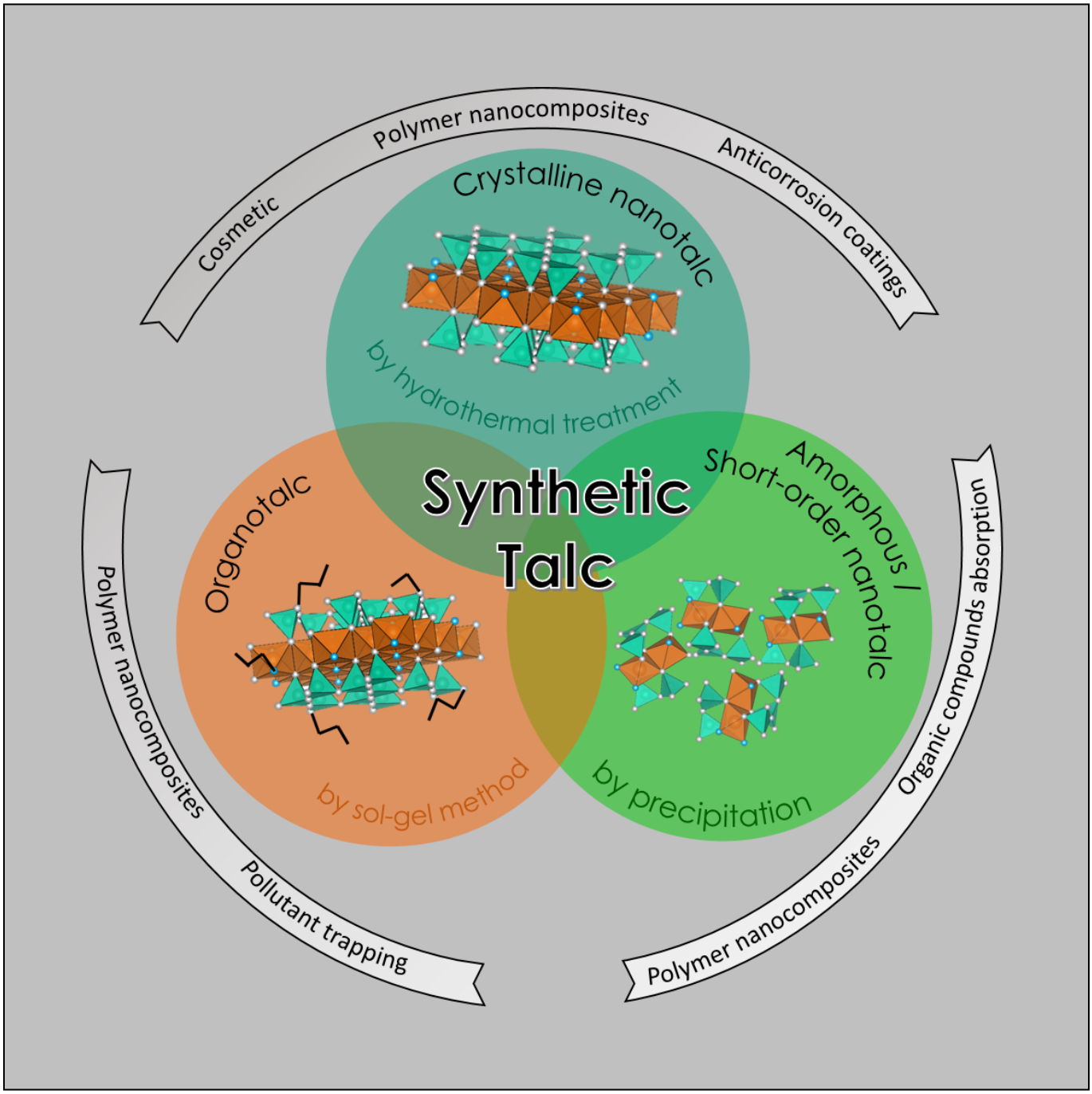

Abstract: This paper gives a comprehensive review about the progress in preparation methods, properties and applications of different synthetic talc natures: i) crystalline nanotalc synthesized by hydrothermal treatment; ii) amorphous and/or short-range order nanotalc obtained by precipitation and iii) organic-inorganic hybrid talc-like structures obtained through a sol-gel process or a chemical grafting. Several advantages of nanotalc such as high chemical purity, high surface area, tunable submicronic size, high thermal stability, and hydrophilic character (leading to be the first fluid mineral) are emphasized. Synthetic nanotalc applications are also considered including its use as nanofiller in composite materials, as absorbers of organic compounds, as anti-corrosion coatings and as agent for cosmetic applications. Regarding their high industrial application potential, intensive research has been carried out to better understand their behavior and develop processes to produce them. To facilitate further research and development works, scientific and technical challenges are discussed in this review paper.

1. Introduction

Clays are abundant and cheap resources distributed worldwide, which find applications in many different fields. Clays are usually used as mineral fillers in ceramic, polymer, paper, cosmetic, pharmaceutical, oil drilling and isolation industries.[1] Clay minerals belong to the phyllosilicates group and can be classified as T-O (1:1), T-O-T (2:1) or T-O-T-O (2:1:1) phyllosilicates based on the arrangement of tetrahedral silicate sheets and octahedral hydroxide sheets.[2,3] Among T-O-T phyllosilicates, talc is the less complex with the formula $Mg_3Si_4O_{10}(OH)_2$.[4]

Talc is known from the Antiquity for its softness and its whiteness in powder form[5] and was first named in 1546 by Georgius Agricola.[6] Talc deposits are the result of the transformation of preexistent magnesian rocks (dolomite, magnesite or serpentinite) or siliceous rocks (quartzite or pelite), by hydrothermal circulations carrying components necessary to the formation of minerals such as MgO, SiO_2, CO_2 and H_2O.[7] The conditions requested for its formation are those of a metamorphism (due to changes of pre-existing rocks under pressure and temperature) of low intensity, i.e. at temperatures of about 350°C. The broad spectrum of talc formation conditions explains the diversity of talc ore deposits all over the world. Thus, talc ore has to be described in term of color,[8,9] grain size, crystallinity, lamellar-character, softness, chemical composition and the accessory minerals such as chlorite and carbonates.[10,11] Talc is a monoclinic and/or triclinic mineral[12] with a density between 2700 and 2800 $kg.m^{-3}$.[13] It is composed of neutral layers stacking, bonded together only by weak van der Waals interactions (Figure 1). The interlamellar distance is 9.33 Å and the energy necessary to the displacement of the layers was quantified about 4 $kcal.mol^{-1}$.[14,15] An elementary layer is composed of a sheet of linked [$MgO_4(OH)_2$] octahedra (''O'') sandwiched between two sheets of SiO_4 tetrahedra combined to six-member rings (''T''), giving the so-called ''T–O–T''-layered structure (Figure 1).[15–17] Within the layer structure, atoms are linked by covalent bonds. The basal faces of the layers account for 90% of the total surface[18] and do not contain hydroxyl groups or active ions contrary to the lateral faces that contain few –SiOH and –MgOH groups. Lateral surface, more reactive,[19] presents a Brönsted acidity whereas basal surface of talc, consisting of Si-O-Si siloxane bonds, presents a low character of a Lewis basicity. Because of the lamellar geometry, the predominance of hydrophobic basal surfaces explains the difficult dispersion of a natural talc in aqueous medium.

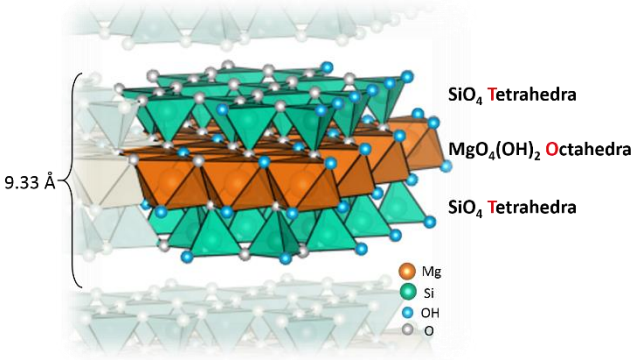

Figure 1. Crystal structure of talc (2:1 phyllosilicate) – 1 elementary layer = T-O-T + Interlayer space. Reprinted with permission from ref [20].

Like the hydrophobic character, the talc lamellar structure described above explains the intrinsic properties of this mineral such as its lubricant character, its chemical inertness, its adsorption properties or its high thermal stability up to 900°C. Its lubricant character (or its softness and its low-hardness) originates from the weak binding forces between talc layers. Talc is at the origin of a wide range of application as shown in Figure 2. Talc is used as mineral filler in various industries to reduce production cost and/or gain new properties. As example, for its high thermal stability, talc is used as a refractory material in kiln furniture; for its neutral electric charge, it is used as an electrical and thermal insulator material in composites. For its platy shape, talc is dispersed in polymer to increase the stiffness, the heat resistance and barrier properties to reduce shrinkage.[21] For most of these applications, talc is used as a fine powder.

[a] M. Claverie, C. Careme
Imerys, 2 place Édouard Bouillières, 31100 Toulouse, France
[b] Dr. A. Dumas, M. Poirier, Dr. C. Le Roux, Dr. P. Micoud, Prof. F. Martin
Geosciences Environnement Toulouse (GET)
UMR 5563, UPS-CNRS-IRD-CNES, ERT 1074 Géomatériaux
14, Avenue Êdouard Belin, 31400 Toulouse (France)
E-mail: francois.martin@get.omp.eu
[c] Dr. C. Aymonier
CNRS, Univ. Bordeaux, ICMCB, UPR 9048, 33600 Pessac (France)
E-mail: cyril.aymonier@icmcb.cnrs.fr

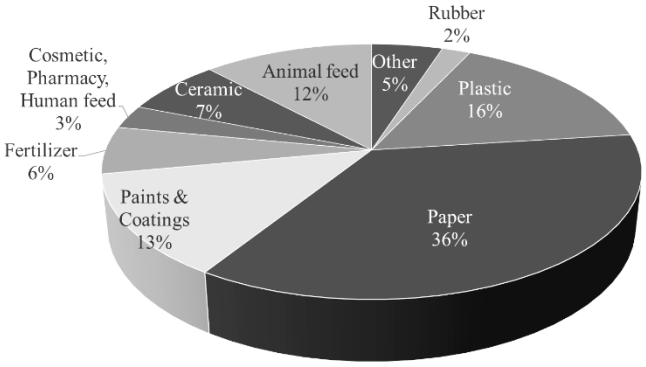

Figure 2. Distribution of talc uses in industry (data for 2013).[22]

However, throughout talc applications, new requirements and/or new limitations appeared such as (i) the need of talc ore purity, particularly in cosmetic and pharmacologic uses ; (ii) the difficulty to disperse talc in an aqueous medium;[23] and (iii) the need to use submicronic talc particles to develop polymer based nanocomposites (first polymer/clay nanocomposites have been reported in pioneering work by a group at Toyota in 1993).[24–27] To satisfy these respective requirements, possible ways were put forward: (i) the need of high purity talc was solved by the exploration of new highly pure talc deposit[28,29] and/or the improvements of techniques to purify talc ore deposits;[30] (ii) talc dispersion in an aqueous medium was improved by using surface-treatment such as pre-coating by carboxyl methyl cellulose adsorption for example;[31–33] and (iii) the need of submicronic talc particles led to the development of grinding processes such as air jet milling,[34,35] sonication,[36] stirred ball milling[37] and dry milling.[38] Alternatively, the company Nanova has developed a mechanical-chemical process to reduce particle size and increase the surface area of talc.[39] However, using these top-down approaches, the results were not as successful since natural talc is difficult to ground homogeneously below 1 µm without leading to amorphization and structural disordering.[40,41] In this context, in the aim to obtain the combination of the three needs (purity; nanosize without amorphization of the structure and hydrophilic character), bottom up approaches have been investigated in the last 20 years.

This review aims to describe the different natures, synthesis methods and applications of nanotalc. Three nanotalc natures are found in literature and differ by synthesis methods, structural order and composition. So, this review is divided in three parts according to these nanotalc (Figure 3). The first one concerns the synthesis of crystalline nanotalc using hydrothermal treatment since it has been the first method historically used by geoscientists. The second one deals with the study of the amorphous nanotalc, also called short-range order nanotalc. As regards the third part, different organic-talc like structures will be detailed. For each nanotalc nature, an overview of the synthesis methods is described, followed by characterization, properties and application of these synthetic materials. Synthetic talc mineral with high purity and well-designed structure is a new route towards advanced functional material which aim at developing new applications.

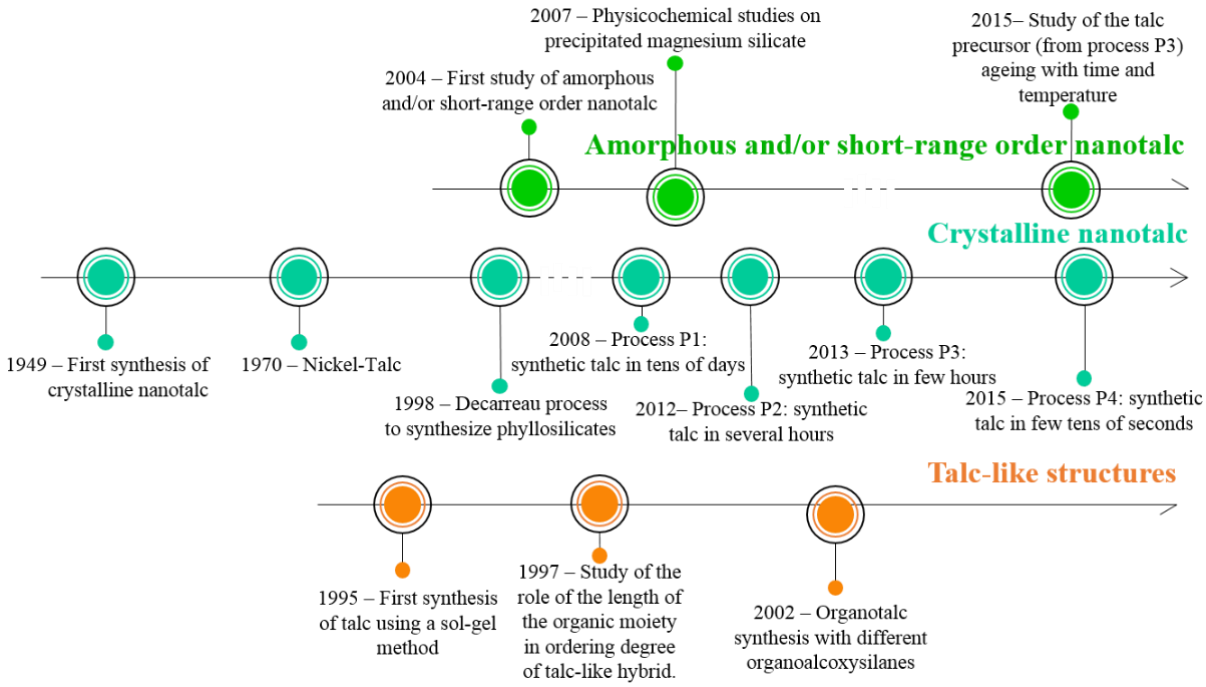

Figure 3. Historical timeline of the synthesis method of nanotalc.

Marie Claverie is currently a Ph.D. student working on the continuous preparation of synthetic talc in supercritical water. She received her M.Sc. degree in Materials Science from Toulouse University (France) in 2014. Her Ph.D. project is based on a collaboration between the IMERYS group, the group of Dr. Cyril Aymonier (ICMCB, Bordeaux) and the group of Prof. FranÅois Martin (GET, Toulouse). Her research interests are focused on the near- and supercritical hydrothermal synthesis of phyllominerals.

Angela Dumas is currently associated researcher at the University of Brasilia (Brasil). After conducting her Ph.D. research in geoscience at the University of Toulouse, France (GET, Geomaterial group), she explored material chemistry through a postdoctoral positionat the INIFTA (La Plata, Argentine) and the ICMCB (Bordeaux, France). Her research is at the interface between materials science and earth sciences and is focused on natural and synthetic clay minerals and clay-based materials.

Christel Carême is Technical Market Manager for IMERYS. She has a Master's degree in industrial process. She is in charge of new product development in several applications and manages a team of five development engineers. She is also in charge of a global and strategic project for IMERYS: the development of synthetic minerals.

Mathilde Poirier is a Ph.D. student at the GET laboratory of Toulouse (France). She is currently working on the preparation of new organic–inorganic hybrids based on synthetic phyllosilicates and she investigates the adsorption mechanisms occurring at the organic–inorganic interface.

Christophe Le Roux is CNRS researcher at the Laboratoire Géosciences Environnement Toulouse (GET, France). His main research interests are mineral synthesis of nanostructured materials through solvothermal synthesis and their functionalization, organometallic catalysis (bismuth chemistry) and organic chemistry (green chemistry).

Pierre Micoud is research engineer at Toulouse University (GET, France). After studying geology he obtained a Ph.D. degree in materials science. He works on the technical development of synthetic clay structures and has been the patent referent in the geomaterials group directed by François Martin for the past eleven years.

François Martin is full Professor of mineralogy and crystal chemistry at Toulouse University (France). He obtained his Ph.D. degree in Physical Chemistry from the Aix-Marseille University (France) in 1994. He is the pioneer of the nanomineral syntheses and the "father" of "mineral fluids". He is currently working on the insertion of minerals into composites with various companies. He is also laureate of many prizes in innovation, and the head of the geomaterials group.

Cyril Aymonier is CNRS senior researcher at the Institute of Condensed Matter Chemistry of Bordeaux (ICMCB). His current research interests are the study of the chemistry and nucleation and growth in supercritical fluids applied to the design of advanced and multifunctional nanostructured materials, the study of materials recycling using supercritical fluids, and the development of associated technologies. He is head of the department "Supercritical Fluids" of ICMCB.

2. Crystalline nanotalc obtained by hydrothermal treatment.

This chapter deals with the talc synthesis using hydrothermal treatment and provides a better understanding of the needs of researchers to mimic nature at a nanoscale. It runs through the history and the advancement of synthetic talc processes. The first aim to synthesize talc was to answer fundamental geological questions, then, synthetic talc stimulated interests of material scientists to develop innovative geo-based materials.

2.1. Evolution of synthesis method for crystalline nanotalc.

2.1.1. Synthetic nanotalc obtained by conventional hydro-thermal synthesis.

From milligrams for Geosciences studies…

Synthesis of talc was firstly reported by geoscientists in chemistry with the aim to better understand geological formation mechanisms of clays. In the 50s, synthetic talc was the result of phase equilibria studies in the systems $MgO\text{-}SiO_2\text{-}H_2O$ and $MgO\text{-}Al_2O_3\text{-}SiO_2\text{-}H_2O$ at high temperatures and high pressures. These experiments were conducted to understand the stability of metamorphic minerals and mineral assemblies. These syntheses were achieved thanks to the simultaneous development of equipments able to support high pressures and high temperatures such as the *Tuttle apparatus*[42] or the *test-tube bomb.*[43] In this context, Bowen and Tuttle performed the first synthesis of talc in hydrothermal conditions from $MgO\text{-}SiO_2\text{-}H_2O$ at temperatures up to 1000°C under pressures between 100 and 280 MPa, for synthesis durations between few hours to few days.[44] These first results showed that talc was formed at temperatures lower than 800°C under pressures comprise between 40 and 200 MPa. Few years later, in 1955, the study of the system $MgO\text{-}Al_2O_3\text{-}SiO_2\text{-}H_2O$ led to synthesis of talc under milder conditions.[45] Talc was synthesized in 20 days at a temperature between 275 and 300°C, under a pressure around 69 MPa. In 1969, Johannes showed that the lowest limit of talc stability was 320°C in the system $MgO\text{-}SiO_2\text{-}H_2O\text{-}CO_2$.[46]

In parallel with these phase equilibrium studies, Wilkins and Ito synthesized a wide range of talc composition with different octahedral cations such as Ni^{2+}, Co^{2+}, Fe^{2+}, Mn^{2+} and Zn^{2+} to understand the effect of octahedral substitution in talc on infrared spectroscopic signals.[47] To do so, the authors prepared first a silico-metallic precipitate from a mixture of sodium silicate and magnesium hydroxide or metallic carbonate; then, the precipitate was put in a stainless steel autoclave at temperatures comprises between 680 and 700°C, under pressures between 200 and 300 MPa, for 15 to 72 hours.

In 1970, nickel-talc was synthesized by mixing silicon dioxide and nickel hydroxide and by treating hydrothermally the precipitate at 350 °C for 120 h in a stainless steel autoclave.[48] Nickel talc was synthesized to study thermal decomposition and the reduction of nickel silicate to develop nickel catalyst on silicate.

In 1982, magnesium silicate mineral derived from the talc-water system in hydrothermal conditions were studied by Whitney and Eberl.[49] The hydrothermal treatments of a gel precursor of talc were realized into a tiny autoclave lined with gold at temperatures between 300 and 550 °C, for synthesis duration varying from 7 to 200 days, at a constant pressure of 100 MPa. The authors showed that talc precursor was transformed in talc after 7 days whatever the temperature. However, they reported that after 7 days of synthesis at a temperature between 300°C and 450°C, the obtained talc was not stable with time and was degraded progressively into stevensite (a T-O-T phyllosilicate with a negative charge layer and with the formula $Mg_{3-x}Si_4O_{10}(OH)_2.nH_2O$). On the other side, at a temperature over 500°C, talc crystallinity was improved with synthesis time and no mineral transformation was observed.

Simultaneously, mineral synthesis was a tool to understand formation mechanism of clays and soils. In this way, at the end of the 80s, Mondésir[50] and Decarreau[51] put in evidence clay phase transition as function of temperature: stevensite/kerolite (mineral with formula $(Mg,Fe,Ni)_3Si_2O_5(OH)_4$) and kerolite/talc. Decarreau *et al.*[51] demonstrated that the stability of the mineral depended on the temperature of the hydrothermal synthesis and concluded that the starting temperature for talc crystallization was approximately 170°C. However, this method led to an unstable synthetic talc, as observed in a retromorphosis experiment during which the crystallinity decreased to form kerolite.

Later, in the 90s, based on the Decarreau process,[51] Martin *et al.* synthesized phyllosilicates in which the tetrahedral and octahedral cations were partly or wholly substituted by germanium and gallium or nickel and cobalt, respectively.[12,52–54] These studies aimed to access the insertion possibilities of these elements in phyllosilicates to obtain crystallographic and crystal-chemistry data. An increase of crystallinity was observed in substituted talcs without any modification of the symmetry group in the crystal lattice.[52,54]

The synthesis of talc described by Decarreau *et al.* offers the mildest synthesis conditions (80–240 °C) and was used further as a reference synthesis.[51] For this reason, the protocol followed by Decarreau *et al.* is detailed below. The synthesis starts with the formation of a precipitate obtained from the mix between a solution of sodium metasilicate and magnesium chloride with a Mg/Si identical to that of talc (i.e., 3/4). The precipitation reaction is:

$$4(Na_2SiO_3) + 3(MgCl_2) + 2HCl + mH_2O \rightarrow Si_4Mg_3O_{11},nH_2O + 8NaCl + (m\text{-}n+1)H_2O$$

with m and n entire numbers.

The precipitate is cleaned to take away the NaCl salt and dried at 60°C during three days. A trituration process is then necessary after drying because of the formation of a solid agglomerate. Then, the obtained powder is dispersed in water and the suspension is introduced in a metallic autoclave lined with polytetrafluoroethylene (maximal stability temperature: 240 °C). The synthesis is performed at 240°C, under autogenous water pressure (1.6 MPa), for 15 days to 30 days.

Since the work of Decarreau *et al.*,[51] the talc synthesis evolved significantly and known a resurgence of interest due to potential applications in material science leading to a production from few

milligrams to few grams between 1989 and 2013. Figure 4 reports the evolution of synthetic talc processes.[55]

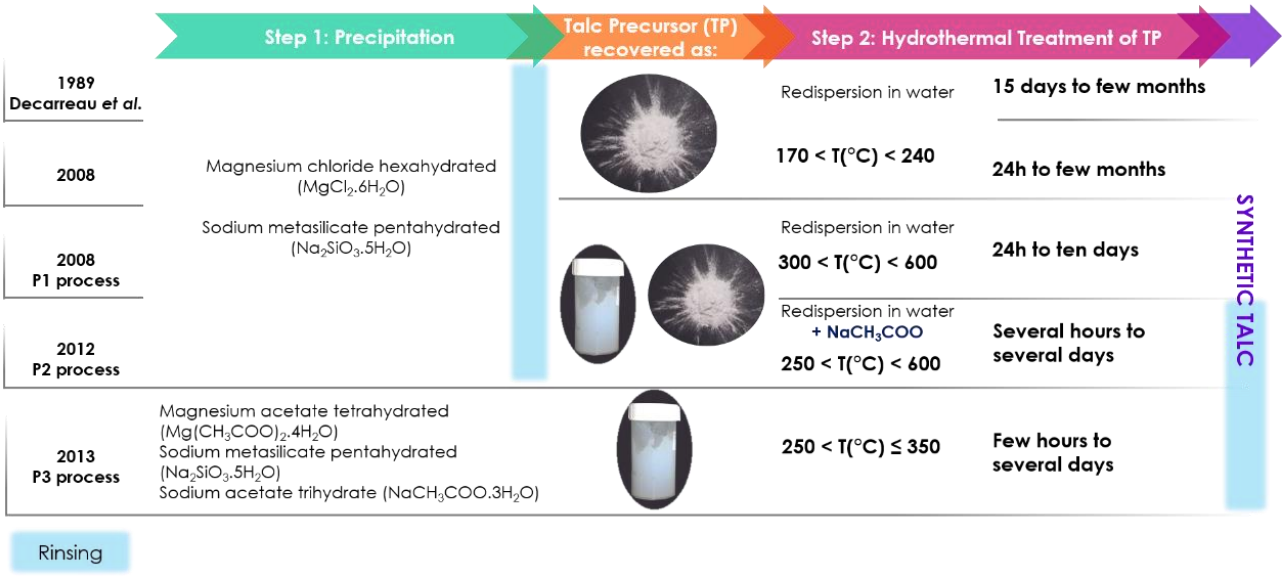

Figure 4. Evolution of the hydrothermal talc synthesis process. Reprinted with permission from ref [55].

… to tens of grams for material investigation.

Decarreau *et al.*[51] works were used in material research as a starting point for the synthesis of nanotalc. All the synthetic talc preparations described below required at least two steps: 1) the formation of a talc precursor (it results from the mixture of a source of silicon and a source of magnesium in a ratio corresponding to the stoichiometric ratio of talc: 4 silicon atoms for 3 magnesium atoms) and 2) the hydrothermal treatment of this talc precursor in an autoclave.

As the method described by Decarreau *et al.*[51] did not lead to a stable product, the first patented process described how a stable talc composition could be obtained from a synthetic kerolite through annealing, for example, at 550 °C for 5 h.[56] Although this process allowed obtaining talc particles, this process was still long and tedious.

Lèbre[57] led to a significant process evolution by studying the influence of various synthesis parameters such as the reactants, the drying method, the temperature, the pressure, the synthesis duration, or the solid/liquid ratio introduced into the reactor. To perform a hydrothermal treatment at higher temperatures (300-600°C), autoclaves in titanium or Hastelloy instead of Teflon-coated were developed. This process, referred as P1, eliminates the step of drying and grinding before the hydrothermal synthesis, reduces the hydrothermal treatment step from months to weeks, and does not require the annealing step of the former process (Figure 4).[57,58] The reactants used in the P1 process were identical to the ones used by Decarreau *et al.*[51] These syntheses were made at a small scale (0.35 L or 2 L), the process was then developed at a larger scale (18.5 L autoclave reactor) to produce few hundred grams instead of few tens of grams (Figure 5). The synthesis scale-up did not require further process modifications. The process was reliable whatever the volume of the autoclave for similar synthesis conditions.

In the 2012s, the synthetic talc process evolved allowing to reduce the hydrothermal treatment step from weeks to a few days (Figure 4).[59] The innovation was based on the addition of a carboxylate salt to the talc precursor before the hydrothermal treatment. The formula of this salt carboxylate is R-COOM, where M is either Na or K, and where R is either H or an alkyl group having less than ten carbon atoms. In this process, named P2, the precipitation step is identical to that described in P1; the novelty occurs before the hydrothermal treatment when the precursor (powder or gel) is dispersed in a carboxylate salt solution; then, the mix is introduced in the autoclave and the hydrothermal treatment was commonly performed at 300°C, under an autogenous water pressure (8.5 MPa) in a titanium autoclave whose the cover sealing is ensure by a graphite seal; after the hydrothermal treatment, talc in the form of gel is separated from the salt solution through successive centrifugation cycles. Several salts were tested such as sodium formate (HCOONa), potassium acetate (CH_3COOK), sodium acetate (CH_3COONa) and sodium butyrate (CH_3-CH_2-CH_2-COONa). Figure 6 compares the XRD patterns of talc synthesized with these different carboxylate salts. Finally, sodium acetate was chosen for its low cost, its harmlessness for human and environment and its stability during the hydrothermal treatment.[60–62] Moreover, the use of sodium acetate led to a gain of talc crystallinity.

Figure 5. A 18.5L stainless steel autoclave used for the preparation of P3-nanotalc (GET laboratory, Toulouse, France; Parr Instrument Company; property of Imerys Talc Europe).

Although the process P2 improved the kinetic of transformation of the talc precursor into crystalline talc, it complicated the process by the addition of talc precursor into a salt solution. In this context, the process named P3, which was aimed to keep "the catalytic effect" of the carboxylate while optimizing the process, was developed. [63] The novelty of this process was in the precipitation step and more precisely in the change of the reactants and the mix procedure (Figure 4).[55,64] The change of the magnesium source from magnesium chloride to magnesium acetate and the precipitation with sodium metasilicate allow the production of sodium acetate as follow:

$4(Na_2SiO_3) + 3(Mg(CH_3COO)_2) + 2(CH_3COOH) + mH_2O + yCH_3COONa \rightarrow Si_4Mg_3O_{11},nH_2O + (8+y)CH_3COONa + (m-n+1)H_2O$

with m, n and y entire numbers.

Contrary to P2, the cleaning step after talc precursor precipitation is removed and the gel obtained is directly introduced in the autoclave to undergo the hydrothermal treatment. The synthesis is performed commonly at 300°C under an autogenous pressure of water (8.5 MPa) in a titanium autoclave as previously described. After the hydrothermal treatment, the gel of talc is separated from the solution of sodium acetate by centrifugation and is cleaned. Synthetic talc can be recovered as a gel or as a dry powder. The P3 process in addition to simplify the synthesis procedure presents the advantage to reduce once more the hydrothermal treatment duration from a day down to few hours. Using the P3 process, the influence of several synthesis parameters (reaction time, temperature, pH, addition of sodium acetate, pressure) on the talc crystallinity was investigated by Dumas *et al.*[55]

To conclude, the process evolution of talc synthesis by hydrothermal treatment is time-saving since it simplifies the synthesis steps and reduces significantly the hydrothermal treatment duration. To obtain a synthetic talc having a similar crystallinity using P1, P2 and P3 processes, 21 days are necessary using P1, against 24 hours using P2 and only 6 hours with P3 (Figure 7).

The P3 process was also adapted for the synthesis of substituted talcs. Talcs with nickel, cobalt, zinc, manganese, copper and germanium were produced. While in the octahedral sheet cobalt and nickel can substitute entirely magnesium, substitutions by zinc, manganese and copper are limited.[65] When nickel or cobalt wholly replace magnesium atoms in the talc structure, an increase of talc crystallinity is observed. A study was carried out to evaluate the benefits of low insertions of divalent or trivalent cations in the talc structure. The cationic insertion was considered as a tool to increase talc crystallinity or to reduce synthesis durations.[65]

To resume, since 2012, the process of synthetic obtaining talc was revisited with the aim of making it compatible with industrial requirements in terms of yield and cost-effectiveness. The evolution of the synthesis protocol made it possible to reduce considerably the synthesis time from several days down to only few hours. Always with the aim of increasing the productivity of synthetic talc, an alternative way of heating was tested: heating by microwaves.

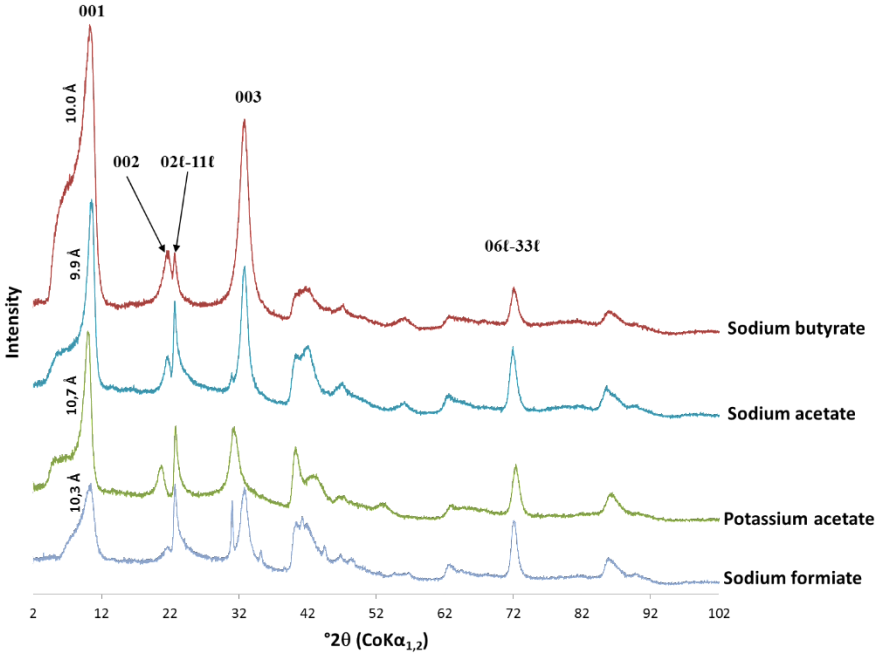

Figure 6. XRD patterns of synthetic talc obtained with the P2 process using different carboxylate salts (1 M solution). Reprinted with permission from ref [65].

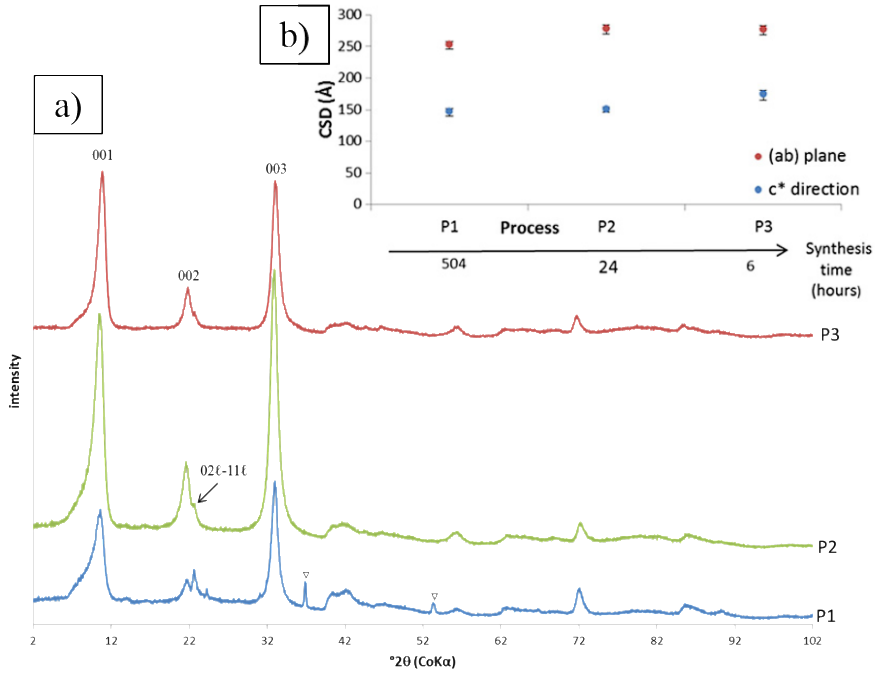

Figure 7. a) XRD patterns of synthetic talc from processes P1, P2, and P3 (∇: NaCl) with the same crystallinity (about 160 Å in the c* direction and 270 Å in the (ab) plane). The synthesis temperature was 300 °C, and the related autogenous pressure was approximately 8.5 MPa; synthesis times were 21 days, 24 h, and 6 h for P1, P2, and P3, respectively – b) Coherent Scattering Domain (CSD) sizes in the c* direction and (ab) plane as function of the talc process. Reprinted with permission from ref [55].

2.1.2. Microwaves-assisted synthesis of talc.

To optimize the process of talc synthesis, the microwave radiations route was tested using the P3 protocol. The hydrothermal treatment was performed in a 100 ml Teflon reactor in a Milestone Start D microwave furnace by varying synthesis duration from one minute to few hours. Due to the microwave reactor material used, synthesis temperature was restricted to 230°C (500 W). Microwave hydrothermal treatment at 230°C provides a rapid structuration of the talc precursor into crystalline talc. This result was supported by XRD, XRD simulations, NMR and FTIR data. This experimental approach of talc synthesis using an alternative heating route indicates that talc structuration can be a rapid process. One minute under microwave radiation is enough to obtain a talc comparable in the c* direction to the one obtained by conventional heating during several hours (Figure 8). Moreover, as synthesis duration did not influence crystallinity, these experiments demonstrated that synthesis temperature is a key parameter to growth the talc in the c* direction.

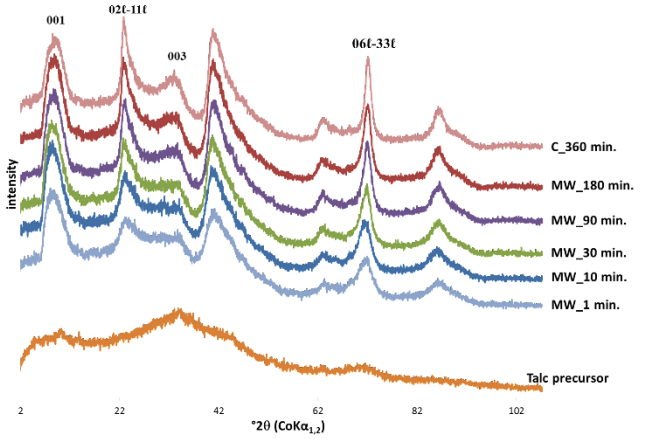

Figure 8. XRD patterns of synthetic talcs obtained by microwaves (MW) heating at 230 °C under autogenous vapor pressure for synthesis time varying between 1 to 180 minutes. MW-talc samples are compared to a talc precursor and synthetic talc obtained using a conventional heating system at 230°C for 360 minutes. Reprinted with permission from ref [65].

However, hydrothermal synthesis research by microwave heating did not go further because of scale-up difficulties of batch reactor using microwaves radiation.[66] In addition, temperature limitation due to the non-existence of microwave-transparent material stable at temperature of 300°C was an obstacle to talc crystallinity.[65] In the objective to always adapt the protocol of talc synthesis to the requirements of an industrial production, the supercritical hydrothermal synthesis in continuous flow was investigated.

2.1.3. Continuous synthesis of talc in supercritical water.

Hydrothermal nanotalc received an industrial interest which was a driving-force to investigate new scalable synthesis solution. This part deals with the innovative route to synthesize talc using supercritical water (SCW). A fluid is said in supercritical conditions when it is processed above its critical temperature (T_c) and above its critical pressure (P_c). Working in the supercritical domain offers the possibility of a continuous change from the liquid phase to the gas phase: density, viscosity and diffusivity can be finely tune between those of a gas and a liquid.

Supercritical water is a good candidate to be used as supercritical fluid. The phase diagram of water is presented in Figure 9. SCW is cheap, non-toxic, non-flammable, non-explosive and used as a "green" solvent. The properties of water drastically change around the critical point (T_c = 374 °C, P_c = 22.1 MPa and ρ_c = 322 kg.m^{-3}) (Figure 9b). The reduction in water density and dielectric constant (ε) seen between room conditions and the critical point (from ε ≈ 80 to ε ≈ 6) has important consequences for the water solubility of compounds [67] (organic compounds become highly soluble [68] whereas the solubility of inorganic salts is strongly reduced). The drastic fall in water density at the critical point has an impact on the water structure at the microscopic scale and thus, on solvation mechanisms, solubility and reactivity (also on the fall of the dielectric constant). Moreover, the decrease of the ionic product of water will change the hydrogen ions (H+) and hydroxide ions (OH-) concentration and thus, the acido-basic processes.[69]

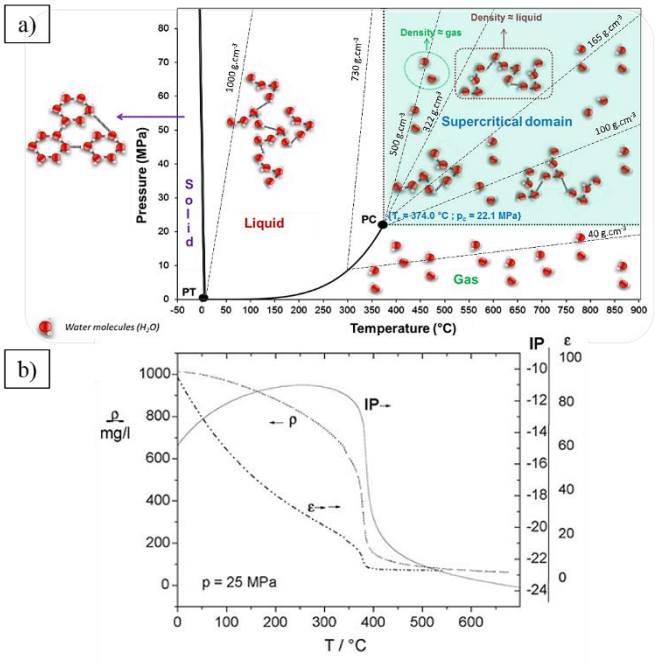

Figure 9. (a) Pressure-temperature phase diagram of pure water. PT is the triple point (T_{PT} = 0°C, P_{PT} = 0.612 MPa) and PC is the critical point (T_{PC} = 374°C, P_{PC} = 22.1 MPa). Some isochoric curves are drawn (dotted lines). Reprinted with permission from ref [70] – (b) Evolution of density (ρ), ionic product (IP) and dielectric constant (ε) of the water as a function of the temperature. Reprinted with permission from ref [68,71].

Industrially, supercritical fluids are mainly used in extraction processes[72] but also in the domains of the environment,[70] energy[73] and cleaning.[74,75] Supercritical fluid (for instance supercritical carbon dioxide) for synthesis of metal particles has also been subject to increasing consideration.[76–80] Since a few decades, supercritical water found innovative applications in inorganic nanomaterials synthesis.[81–86] In the early 90s, Adschiri and coworkers were the pioneers to use this method to synthesize cerium oxide nanoparticles.[84] The nanoparticle design in terms of size, morphology, structure, composition and crystallinity can be controlled by varying water properties adjusting temperature and pressure.[81,87,88] Several publications highlighted the advantages of this process for the processing of nanomaterials.[70,81,82,87,89,90]

In improving the chemical reactivity,[70,74,91–94] the use of SCW induced a significant reduction time from few hours down to only few tens of seconds. That is the reason why the process described below is today particularly suitable for a scaling up towards industry.[89,91,95] Dumas *et al.*[96,97] highlighted the proof of concept for the talc synthesis combining a continuous set-up and the use of supercritical conditions. For the first time, talc precursor preparation and hydrothermal synthesis are performed in only one step based on process developed by Slostowski *et al.* for the synthesis of cerium oxide.[90,98] The reduction of synthesis steps and the use of supercritical water offers a major technical breakthrough since it allows decreasing the synthesis time from several hours to tens of seconds. Moreover, contrary to the batch P3 process, the continuous flow synthesis in supercritical conditions did not require an excess use of sodium salts. At the tee mixer, talc precursor is formed following the equation:

$$4(Na_2SiO_3) + 3(Mg(CH_3COO)_2) + 2(CH_3COOH) + mH_2O \rightarrow Si_4Mg_3O_{11},nH_2O + 8CH_3COONa + (m\text{-}n+1)H_2O$$

with m and n entire numbers.

Talc has been synthesized using a simple custom-built and continuous supercritical hydrothermal reactor, referred as P4 process and illustrated in Figure 10.

The whole device is designed with a 1/8 in. 316L stainless steel coiled tubing. The heater is a homemade coiled ceramic resistance allowing a control of the temperature up to 500 ± 1°C. A back pressure regulator (BPR – micrometer needle valve - Autoclave Engineers) placed downstream the reactor, allows controlling the pressure in the reactor up to 40 MPa. In this process, the precursor solutions (sodium metasilicate and magnesium acetate solutions) are introduced with the high-pressure pumps and directly mixed at the tee mixer point. At this point, the mixture of precursors precipitated to form the talc precursor entity and sodium acetate. This mixture is then flown into the reactor operating in supercritical conditions where the talc crystallization occurs. The reaction is quenched thermally downstream the reactor with an ice bath and the talc was trapped in a filter while the solvent solution is recovered upon depressurization through the micrometric valve. At the end of the experiment, the filter was disassembled from the process, opened and synthetic talc can be recovered.

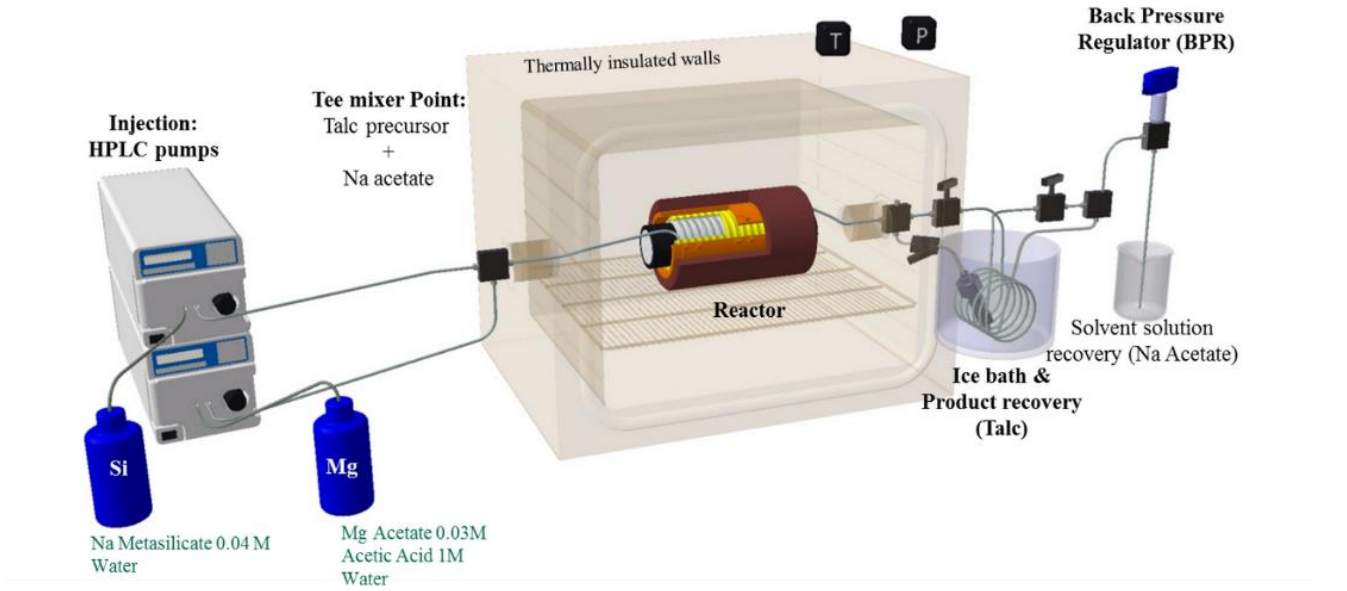

Figure 10. Custom-built continuous supercritical hydrothermal process for talc synthesis. T = thermocouple; P= manometer. Reprinted with permission from ref [96].

Based on this study, a scale-up of the talc synthesis is currently studied. A series of talc was synthesized in tens of seconds in near- or supercritical water using this continuous-flow process (Figure 11). This approach highlights the possibility for a rapid talc structuration (in few tens of seconds) and demonstrates that synthesis time and temperature influence the growth of talc in the c* direction. It should be noted that these XRD characterizations were performed on talc gel directly recovered from the filter and dried without being cleaned. Besides reducing the synthesis time, the absence of salt signals denotes another innovative character of this process: the unnecessary cleaning step of the talc gel.

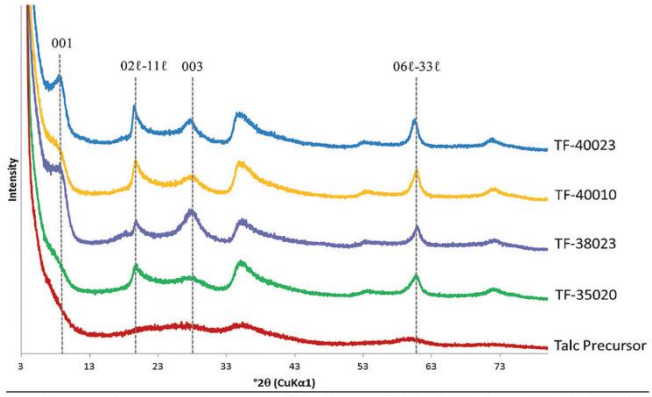

Sample	Reactor	Temperature [°C]	Pressure [MPa]	Synthesis duration [s]	CSD c* [Å]	CSD (ab) [Å]
TF-35020	Continuous	350	25	20–23	46 (1)	94 (2)
TF-38023		380			63 (1)	125 (4)
TF-40020		400			92 (3)	174 (8)
TF-40010				10	70 (2)	132 (5)
Talc precursor	Obtained at room temperature and ambient pressure				amorphous	

Figure 11. XRD patterns of synthetic talc obtained using the continuous near- and supercritical hydrothermal synthesis process for different temperatures (350, 380 and 400°C) and for different synthesis times (10 or 20 seconds). Conditions of synthesis and coherent scattering domain (CSD) measurements. Reprinted with permission from ref [96].

Thus, this study has shown: 1) the possibility to synthesize talc in a continuous flow system; 2) the feasibility of talc in supercritical hydrothermal conditions. This new approach of talc synthesis makes it possible to curtail even more synthesis times. For the first time, talc is obtained in less than one minute. Jointly with the reduction of the synthesis time, this process simplifies the protocol by removing 1) the addition of the sodium acetate during the reaction of precipitation, used as a catalyst of the reaction (P3 protocol), and 2) the cleaning step. This system of production could be the solution for the change of scale necessary for the industrialization.

2.2. Characteristics of crystalline nanotalc.

Synthetic talc prepared using hydrothermal processes (P2, P3 and P4) leads to a product: (1) with a talc-like structure (Figure 7 and Figure 11), (2) with a high chemical purity, (3) with submicronic size, crystallinity or lamellarity defined and (4) with a hydrophilic character (gel of talc).

Synthetic particles from P1 process were characterized using spectroscopic methods (FTIR, NMR). These characterization methods reveal numerous structural defects caused by the synthesis of a biphasic material composed of stevensite-talc interstratified product.[57,99,100]

Contrary to P1, P2, P3 and P4 processes lead to a single-phase product.[55] P3 talcs were extensively studied with various spectroscopic methods (FTIR, NMR), X-ray diffraction and microscopy (SEM, TEM).[64,96] The structural evolution of synthetic talc particles as function of synthesis time was investigated and shows that the synthesis time influences particle size in the (ab) plane.[64,96] The longer the synthesis time is, the bigger the particles are (Figure 12a and b). Moreover, synthesis times between few seconds (continuous process) and few hours (Figure 12c) do not influence particle thickness (< 10 nm).[65] Talc particle size and the number of stacked layers were accessed using AFM and low-pressure argon adsorption analyses (Figure 13).

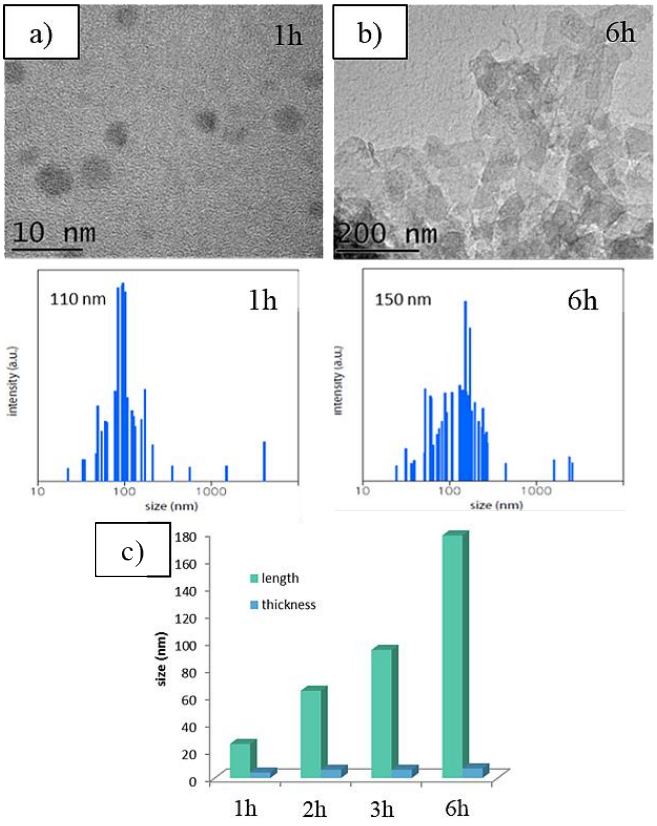

Figure 12. TEM images and size distribution histogram analysis of synthetic talc after (a) 1h and (b) 6h of hydrothermal treatment and (c) evolution of the length and the thickness of particles with synthesis duration (estimated from low-pressure adsorption analyses). Reprinted with permission from ref [65].

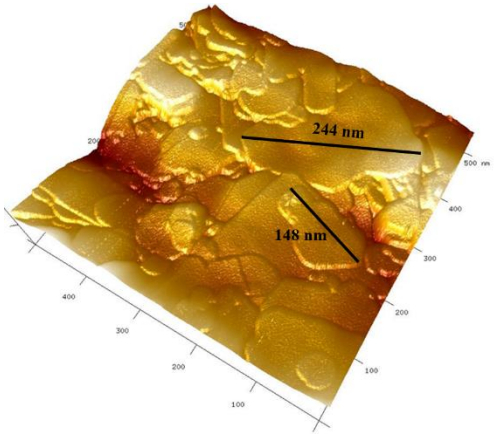

Figure 13. AFM picture of the surface of talc synthesized in 6 h. Reprinted with permission from ref [65].

While synthetic nanotalc and natural micronic talc have the same crystal structure, new spectroscopic signals in NMR and FTIR appear in nanotalc. In ^{29}Si NMR, natural talc is characterized by a broad peak centered at -97 ±1 ppm, that corresponds to silicon in a Q^3 environment (Si surrounded by 3 others Si, in blue in Figure 14). In the case of synthetic talc, in addition to the -97 ppm peak, a signal located at -95 ppm appears and its area decreases with synthesis time while the one at -97 ±1 ppm peak increases. By analogy with crystalline growth observations with synthesis time, this peak at -95 ppm is assigned to a Q^2 environment characteristic of sheet edges (in green on Figure 14).

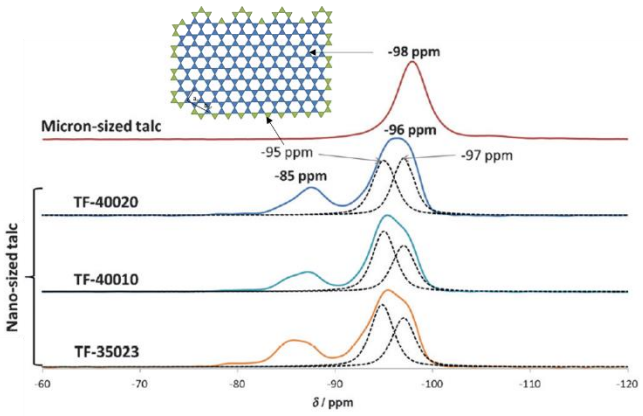

Figure 14. ^{29}Si MAS-NMR spectra recorded on natural talc and synthetic talc. Reprinted with permission from ref [96]. scheme of the talc tetrahedral sheet. Reprinted with permission from ref [65].

Effects of nano size on talc characteristic were also evidenced by ^{1}H NMR spectroscopy. ^{1}H NMR of synthetic talc spectrum reveals three signals at 0.5 ppm, 1.8 ppm and 4 ppm while natural talc is characterized by a broad peak centered at 0.5 ppm and attributed to the structural hydrogen atoms in a trioctahedral Mg environment (Figure 15).[101,102] The peaks observed in synthetic talc samples are assigned to silanols groups on particle edges[102] and physisorbed water at 1.8 ppm and 4.3 ppm, respectively. The hydrophilic character of synthetic talc was also identifiable by FTIR analysis.[64]

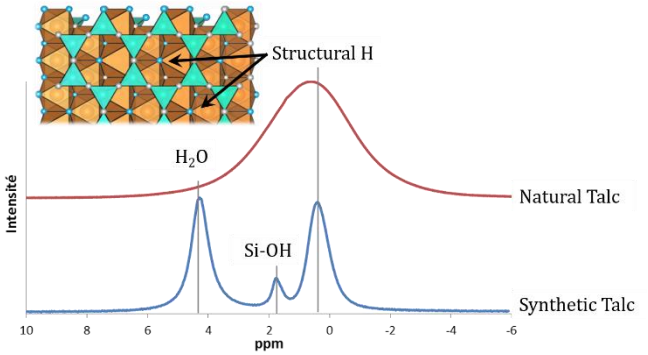

Figure 15. ^{1}H MAS-NMR spectra recorded on natural talc and P3-synthetic talc. Reprinted with permission from ref [65]. Scheme of the talc layer (top view).

Thermogravimetric analyses of natural talc and P3 synthetic powder revealed a high thermal stability up to 800°C (Figure 16). However, unlike natural talc, synthetic talc presents a gradual thermal degradation. This stair-form evolution becomes gradually less pronounced with the growth of particle size. These observations are explained by a progressive dehydroxylation of synthetic talc according to its sizes: the smaller the particle size, the more the OH groups are accessible.[64]

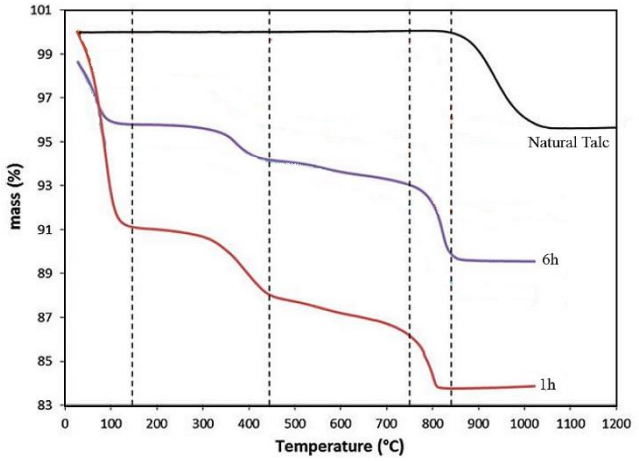

Figure 16. Thermogravimetric curves of P3-talc synthesized in 1h and 6 h. Reprinted with permission from ref [64].

These characterizations of synthetic talc particles allow to observe a growth of particle sizes during the hydrothermal treatment. Particles obtain between 1h and 6h of synthesis meet the objectives which are the monodispersivity and the nanometric character. Spectroscopic analyses allow to identify specific

signatures due to the environments of edge of the particles. So, the longer time of synthesis is, the larger particles are and thus, the less intense characteristic signals of small particles are. The nanometric character brings also a new property: an exacerbated hydrophily. Lastly, these new synthetic talc particles have the advantage of being able to be easily functionalized (magnetism, grafting) with the aim of bringing new properties.

2.3. Functionalization and Applications of nanotalc.

Whereas initially natural talc was introduced into polymer matrixes to reduce the production cost, today nanotalc is studied as a mineral filler to bring new properties and/or functionalities (mechanical reinforcement and barrier properties) to composite materials.

2.3.1. P1-nanotalc.

Lubricant composite material.
The lubricant properties offered by the introduction of P1-nanotalc and micronic natural talc in a metallic matrix (Zn-Ni and Ni-P) were compared by Bonino *et al.*[103] and Etcheverry.[104] Compare to natural talc, P1-nanotalc offers a significant decrease of the roughness and a better dispersion.[104] An international industrial patent was deposited to use P1-nanotalc particles as high temperature lubricant material.[105]

Anti-corrosion coating.
Joncoux-Chabrol *et al.*[99] studied first the incorporation of P1 synthetic nanotalc in a sol-gel coating to improve metal corrosion protection. The barrier property of P1-nanotalc into sol-gel coating were studied and showed an easier dispersion of the synthetic particles, in contrast with natural talc, in the sol-gel matrix. The incorporation of this filler at a concentration of 20 $g.L^{-1}$ greatly enhanced the barrier effect of the coating. However, the long duration synthesis required to obtain P1 synthetic nanotalc (48 hours[106]) did not match with industrial requirements.

Polymer nanocomposite.
Fiorentino *et al.*[107] investigated the influence of both the P1 nanotalc nucleating power and its dispersion rate in a polypropylene (PP) matrix. P1 nanotalc was modified on surface (grafting) and a compatibilizer (a maleic anhydride-grafted polypropylene) was used to develop long-range interactions between filler and matrix.[107] They highlighted an enhancement of the nucleating effect in PP of the grafted nanotalc. Furthermore, by coupling the incorporation of a compatibilizer with P1 nanotalc after organophilic surface treatment, an enhancement of the dispersion and a reduction of the thermal degradation of the filled matrix were observed.[107] Respecting the thermal properties, a higher temperature degradation of synthetic talc polymer nanocomposite was evidenced. This fact is improved by the use of modified synthetic talc.

2.3.2. P3-nanotalc.

The easiest, optimized and most cost-efficient method to obtain synthetic talc is by using the P3 process. As discussed previously, P3 nanotalc has been extensively characterized by several methods.[55,64] For these reasons, the majority of scientific studies are based on the use of P3-nanotalc to meet the needs of industrial applications.

Polymer nanocomposite.
The insertion of P3-nanotalc was studied by Yousfi *et al.*[108] in a nonpolar polypropylene (PP) matrix and in a polar polyamide (PA6) matrix to evaluate its contribution on the mechanical and thermal properties of the composite material. The thermal stability of the P3-nanotalc-filled PP systems is considerably enhanced and the best ductility was observed. For PA6 systems, a good dispersion of P3-nanotalc was possible and a significant increase in Young modulus was highlighted. The authors attributed these phenomena to the high affinity between the hydrophilic synthetic talc and the polar PA6 matrix. Later, the authors used room temperature ionic liquids (RTILs) as effective compatibilizers of PP/PA6/synthetic talc blends.[109] They functionalized P3-nanotalc by two kinds of RTILs based on phosphonium cations. They observed an enhancement of both the thermal properties of PP/PA6/synthetic talc (+80°C) and the mechanical performance without reducing the strain at rupture. They demonstrated a harmonious reaction between ionic liquids and synthetic talc.

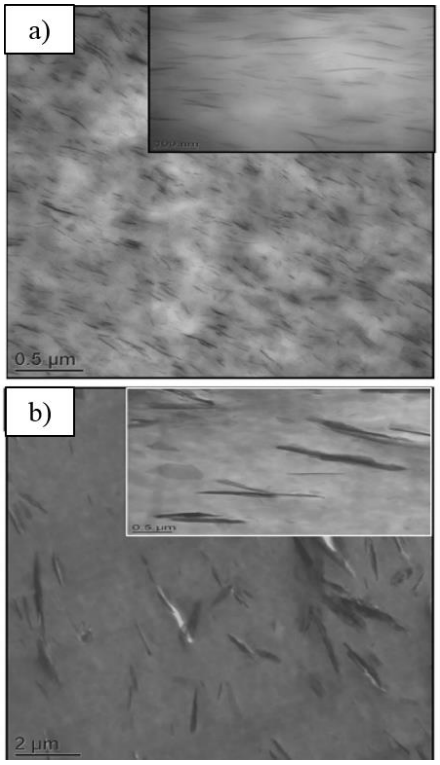

Figure 17. TEM micrographs of (a) PA6/synthetic talc and (b) PA6/natural talc. Reprinted with permission from ref [108]. This figure shows a higher exfoliation and dispersion of synthetic talc in the matrix in comparison with natural talc.

In their study, Beuguel *et al.*[110] introduced P3-nanotalc in PA6 and PA12 matrixes and analyzed the rheological and structural properties of nanocomposites. The results show that P3-nanotalc is better dispersed in PA6 matrix than in PA12 matrix (by reason of the matrix polarity). However, in another study, they highlighted that synthetic talc can be considered as potential challengers of montmorillonite clay, when dispersed in PA12 matrix, since synthetic talcs exhibit a mainly nanometric structure.[111]

As polymeric matrix, the polyurethanes (PU) must be considered because of its different niches of applications, such as coatings, adhesives, foams, thermoplastic elastomers, among others. PU presented good mechanical properties but possess low thermal stability and barrier properties. Prado *et al.*[112] focused on the use of synthetic P3 Ni-talc as filler in the preparation of PU nanocomposites by *in situ* polymerization. They show a good dispersion of Ni-talc in the matrix which is testified by a homogeneous green coloration. So, A great compatibility between filler and polymer is highlighted. This significant dispersion can be explained by several OH interactions of the P3 Ni-Talc with the urethane group of the polymeric matrix. The nanocomposites synthetic Ni-talc/PU noted also an enhancement in thermal stability and of the crystallization temperature in comparison with a composite natural talc/PU or with a pure PU. Figure 18 evidenced that both pure PU and PU/natural talc presented a randomly distribution of the crack growth on the surface. The PU/Ni-talc revealed a rough ordered fractured surface indicating a good dispersion and adhesion of filler and polymeric matrix.

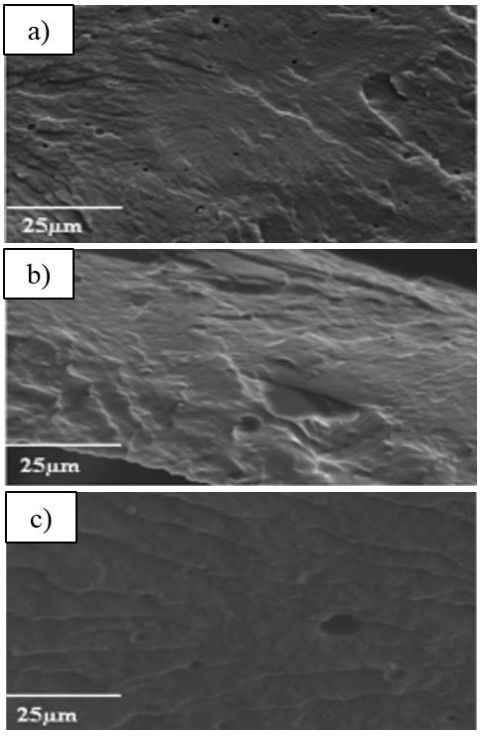

Figure 18. Cryofractured SEM micrographs of (a) pure PU, (b) PU with 3 wt% natural talc and (c) PU with 3 wt% Ni-Talc. Reprinted with permission from ref [112].

Dos Santos *et al.*[113] used new P3 nanotalc associated with nano-Fe_3O_4[114] (Figure 19) as filler for producing magnetic polymeric nanocomposites. The authors revealed a good dispersion of the Fe_3O_4-nanotalc into a PU matrix even at high filler content of 10 wt%. They confirmed the possible use of this filler to obtain magnetic nanocomposites leading to improved materials with high crystallization temperature and thermal stability.[113]

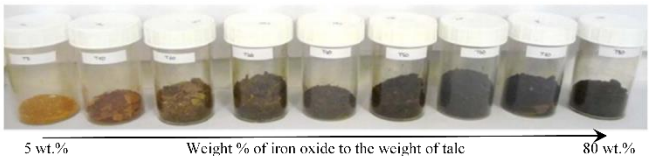

Figure 19. Magnetic synthetic talc ranges obtained. Reprinted with permission from ref [65].

The use of talc as filler in polymeric matrixes is limited by its electrical insulator property (between 10^{-11} and 10^{-16} $S.m^{-1}$). Indeed, it is essential for some applications to have antistatic materials, in particular in the electronic and automotive industry. Fraichard[20] succeeded to confer electrical conductivity to synthetic talc. Fraichard *et al.*[115] modified the synthetic talc through two approaches: the functionalization with carbon nanotubes and the grafting of a conductive polymer (polypyrrole). They obtained a conductive filler about one hundred $S.m^{-1}$. The introduction of these conductive fillers in a low-density polyethylene matrix by extrusion has allowed them to demonstrate that the mechanical properties of the matrix are maintained and its conductive properties are quite improved. These composites may be used as sensors or antistatic parts.

Filler for safety documents.

In 2014, the Arjowiggins Security group patented the use of P3-nanotalc in the production of safety documents.[116] The chemistry control of the synthetic talc during synthesis is the main asset of this material for authentication and/or identification of documents. Synthetic talc is used for its chemistry signatures (tetrahedral and octahedral substitutions) which can be easily and quickly detected by spectroscopic methods such as Raman spectroscopy and near-infrared spectroscopy directly on paper.

Filler for cosmetic application.

In 2014 and 2015, the L'OREAL Group has deposited 14 patents concerning the use of synthetic talc in the form of an aqueous gel in cosmetic formulation. In cosmetic, the purity of synthetic talc is highly assessed, since it prevents the risks of undesirable mineral contaminations. Among the 14 patents, the inventions relate a cosmetic composition for the treatment of skin and nails comprising a synthetic talc and an electrolyte, a polyelectrolyte, a polyol and/or a UV filter.[117–120] The inventions relate also the use of the synthetic talc as an agent for stabilizing a Pickering-type emulsion.[121] Moreover, synthetic talc in the form of powder is patented as a mattifying and homogenizing agent in cosmetic care and make-up.[117,122] Indeed, in cosmetic, it is current to use aqueous gel to stabilize emulsions and dispersion of solid particle

such as filler and pigments. These patents meet the need to propose cosmetic compositions able to convey electrolytes while remaining stable, with a viscosity appreciated by consumers.
Consequently, synthetic crystalline nanotalc illustrates a new filler with highly interesting properties such as a nanoscale, a high purity and a hydrophile character. These characteristics make it attractive in several applications in which natural talc cannot be used. It also must be highlighted that synthetic talc can be easily functionalized opening a wide range of applications.

3. Amorphous and/or short-range order nanotalc.

3.1. Formed at the beginning of precipitation.

The magnesium silicate precipitation research was developed in materials science area with the objective to develop new synthetic fillers. With this aim, Krysztafkiewicz *et al.*[123] realized a parametric study of magnesium silicate precipitation in presence of sodium hydroxide solution. Precipitation was performed by "a drop by drop mixing of solutions of sodium metasilicate and magnesium salts" (chloride, sulfate, and nitrate) at 80 °C (Figure 20a).[123] The presence of a sodium hydroxide solution during the precipitation affected significantly the quality of the obtained magnesium silicate (modification of chemical composition, lower particle size, and higher homogeneity of particle size). Later, Ciesielczyk *et al.*[124,125] proposed three procedures to obtain highly dispersed magnesium silicate (Figure 20b). The authors optimized the precipitation reaction by studying the influence of temperature (20-80 °C), reagent dosing rate, rate of mixing reactants, substrate concentration. Using the procedure III (Figure 20b), a magnesium silicate having the nearest chemical composition of talc was obtained. However, an amorphous magnesium silicate was obtained in form of agglomerate (Figure 21a-b). Ciesielczyk *et al.*[126] studied also the surface modification of synthetic magnesium silicate and the physico-chemical parameters of the obtained product (particle size, bulk density, hydrophobic character).

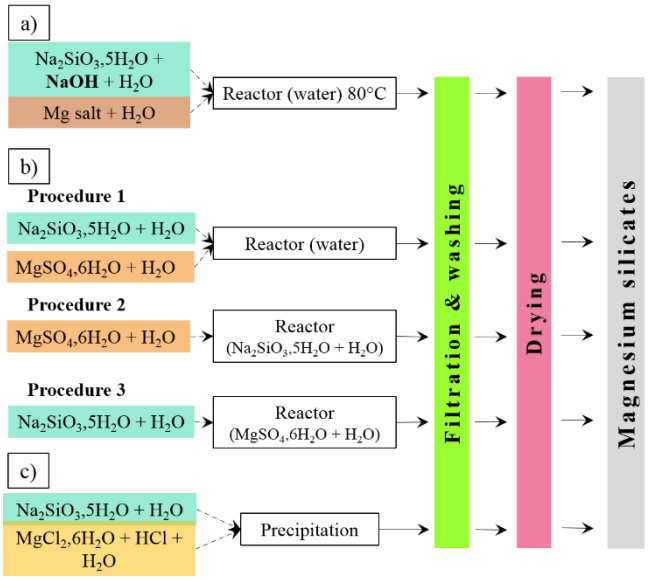

Figure 20. Schemes of the procedure followed to synthesize magnesium silicate according to (a) Krysztafkiewicz *et al.*, (b) Ciesielczyk *et al.* and (c) Dietemann *et al.* Reprinted with permission from ref [123,126,127].

Dietemann *et al.* studied the magnesium silicate precipitation reaction (from the P1 process, Figure 20c)[22,127] which was as follow:

$(Na_2SiO_3) + 3(MgCl_2) + 2HCl + mH_2O \rightarrow Si_4Mg_3O_{11},nH_2O + 8NaCl + (m\text{-}n+1)H_2O$

with m and n entire numbers.

The authors determined the influence of different precipitation parameters (reactant nature, reactant addition, temperature, molarities and ultrasound use) on product properties such as size particle distribution.[127] Dietemann *et al.* described an amorphous and porous structure highly agglomerated Figure 21c-d). An evaluation of the drying process (frying oven, freeze-drying and spray-drying) was also studied to improve particle deagglomeration.

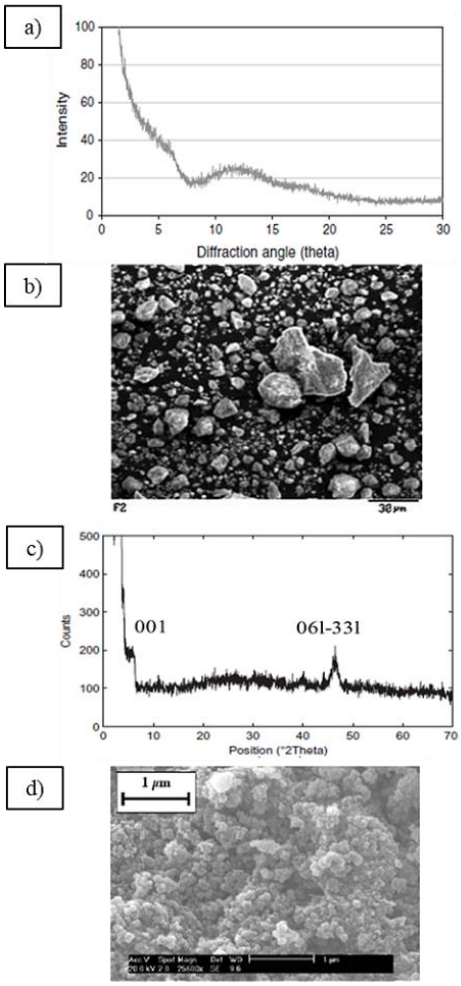

Figure 21. (a) XRD and (b) SEM micrographs of synthetic magnesium silicate obtained by Ciesielczyk *et al.* and (c) XRD and d) SEM micrographs of synthetic magnesium silicate obtained by Dietemann *et al.* Reprinted with permission from ref [125,127].

More recently, in the aim to gain insight into talc crystallogenesis, Dumas *et al.*[65] studied the talc precursor (from P3) ageing with time and temperature by XRD, FTIR and NMR and showed that talc precursor evolves structurally with time in the (ab) plane while the stacking order in the c* direction is limited. Contrary to Lèbre[57] who described talc precursor as a brucite sheet and few polymerized silicon tetrahedra, an EXAFS study showed that Ni-talc precursor was a nanotalc entity; the talc growth unit was constituted by 2−3 Ni-octahedra distanced from each other by 3.07 Å and 3−4 Si-tetrahedra distributed on the top and bottom of the octahedral “sheet” and distanced from Ni by 3.29 Å.[128]

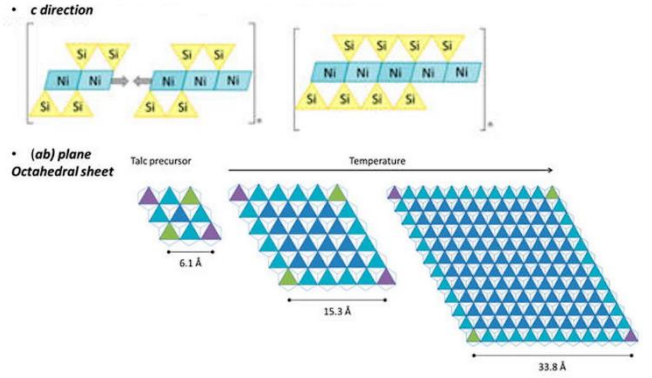

Figure 22. Scheme of the structural evolution of the talc precursor with the temperature in both the c* direction and in the (ab) plane. Reprinted with permission from ref [128].

Simultaneously to the research of magnesium silicate precipitation for developing new materials, basic research on magnesium silicate was developed in cement researches. Magnesium silicate hydrate gels having a Mg/Si ratio of 0.75 was precipitated and characterized by NMR, XRD, FTIR and SEM. This study aimed to offer structural information about this phase that can be formed in cement.[129]

The magnesium silicate material obtained by precipitation is considered as amorphous or as a short-range order material. However, very few information has been carried out on it. Some studies of the effects of process parameters and treatments on solid properties were performed in view to adapt this material for adsorption or reinforcement applications.

3.2. Properties and applications of short-range order nanotalc.

Synthetic amorphous nanotalc was developed to compete with precipitated fumed silica as a filler for the reinforcement of elastomers. It plays a very important role in new products for adsorptive properties.[130] It is speculated that the materials would permit a selective and very effective adsorption, notably for cleaning wastewater of heavy metals and organic compounds.[131]

Absorption.

The works of Ciesielczyk *et al.*[125,131,132] focused on applications of amorphous nanotalc as an adsorbent of organic compounds. Information was gained in the understanding of the effect of some process parameters (temperature, reagent dosing rate, substrate concentration, etc.) and solid treatment (surface modification to introduce functional groups) on properties such as crystallinity, nitrogen adsorption properties and the ability to absorb diverse solvents (water, dibutyl phtalate and paraffin oil).[125] The authors also studied the adsorption of phenol on the surface of amorphous magnesium silicates. Authors showed that adsorption abilities of amorphous nanotalc are mainly due to its high specific area (500 m^2/g) and were not influenced by surface treatment by organofunctional silanes.[132]

In other studies, Ciesielczyk *et al.* highlighted the effects of amorphous nanotalc treatment by non-ionic additives[124] or by silane.[126] All the modified samples became mesoporous after treatment, that increased the surface activity of the solid[124] and so the capacity of absorption of organic solvents (dibutyl phtalate and liquid paraffin).[124,131] This increase of absorption capacity of modified samples was linked with an increase of its lipophilicity what was a considerable advantage for a well-dispersion in a polymer matrix.

Polymer filler.

Amorphous nanotalc was introduced as a filler in several matrixes such as SBR (styrene butadiene rubber)[130] or PP (polypropylene)[22] with the aim to study the mechanical properties of the nanocomposite material. An increase of the Young modulus and the elongation at break was observed when amorphous nanotalc was introduced in SBR matrix.[130] These properties are improved when the amorphous nanotalc is modified with a silane. Regarding the amorphous system nanotalc/PP, a good dispersion of the filler was observed and an increase of the Young modulus and the elongation at break of the nanocomposite material was shown.[22]

Although synthetic nanotalc (after hydrothermal treatment) is a well-studied product, few information about its precursor (amorphous nanotalc) exists. Amorphous nanotalc reveals attractive properties in polymers and absorption. By the same token, the study of its deagglomeration can be viewed in order to prevent the synthetic talc agglomeration.

4. Talc-like structures.

In literature, organic-inorganic hybrid “talc” can be found under the following terms: talc-like structure,[133,134] organic-inorganic talc hybrid,[135–137] talc-like hybrid (TLH) and organotalc.[138] Mainly three methods allow the synthesis of this covalently linked inorganic-organic phyllosilicate: i) the one step sol-gel synthesis, ii) the grafting of organic molecules on talc or iii) the precipitation step with an oxysilane soluble in water.

4.1. The sol-gel process.

The sol-gel process is qualified as “soft chemistry” since reactions occur at ambient temperature. In this process, a sol (or solution) evolves towards a gel-like system containing both a liquid phase and a solid phase.[139] The effectiveness of this process is influenced by several parameters including temperature, pH, nature of solvent used, nature of catalyzer and metallic precursor, as well as the concentration of reagents.[140–142]

Ebelman and Graham[143,144] were the first scientists to show an interest in the sol-gel method for the synthesis of inorganic materials (ceramic and glass) as early as the mid-1800s.[145] The first synthesis of talc by this method was reported in 1995 by Fukushima and Tani.[136] In view of the formation conditions of talc in nature (high pressure and high temperature: 320°C and 250 MPa for the deposit of Trimouns),[146–148] the synthesis of talc at room temperature with a sol-gel process was a challenge. Indeed, in this process, low temperature is required because of the organic nature of the precursor whose thermal decomposition is usually lower than 200°C.[149] Nowadays this method is commonly used, as shown by the number of publication on the subject over the last 10 years (more than 20 published papers).[133,135,150–154]

The synthesis of functionalized talc consists in formulating in a single step a lamellar material whose elementary layer has a TOT structure identical to that of talc. The only difference between natural or synthetic talc and this organo-“talc” is that organic compounds are fixed on silicon atoms of the tetrahedral layers as shown in Figure 23.[137]

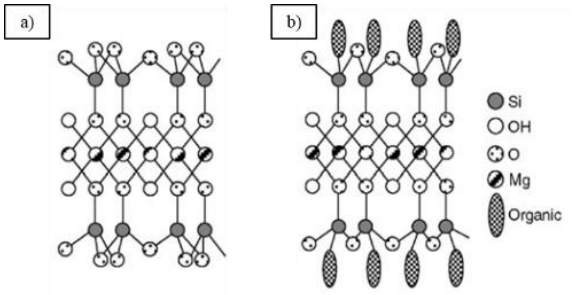

Figure 23. (a) TOT layer structure of a natural talc and (b) Proposed TOT layer structure of an organotalc. Reprinted with permission from ref [137].

Hydrated salts and organo-alcoxysilanes are used as precursors for the octahedral layer and the tetrahedral layers, respectively. Precursors are typically dissolved independently in an alcoholic solution and mixed. During the precipitation, the formation of a hybrid talc occurs by increasing the pH by soda addition.[155–157] The sol-gel synthesis of talc is performed at room temperature for 24h using organotrialkoxysilane ($RSi(OR')_3$) as a silicon source, where R is the organic part and R’ corresponds to ethoxy or methoxy groups.[137] For example, linear alkyl,[158–160] functionalized linear alkyl[134,153,161] and phenyl[162] have been employed for the synthesis of organotalcs (Table 1). This synthesis leads to talc with organic moieties covalently linked to the silicon atoms of the tetrahedral sheets and pending in the interlayer space.[137]

Table 1. Commonly used precursors for the organotalc synthesis with sol gel method

Organosiloxanes	Other compounds	Conditions	Reference
Phenyltriethoxysilane (PTES) (3-mercaptopropyl)trimethoxysilane (TTMS) (3-aminopropyl)-triethoxysilane (ATES) (3-(methacryloxy)propyl)trimethoxysilane (MTMS) Mixtures of Methyltriethoxysilane (MTES) and PTES			Burkett *et al.* [163]
Glycidylpropyltrimethoxysilane (EPTMS) 3-(2-aminoethyl-3-aminopropyl)trimethoxysilane (EDTMS) 1-propenyltrimethoxysilane (ALTMS) Dihydrotriethoxysilylpropyl-1H-imidazol (ITES)	Magnesium chloride hexahydrate Sodium Hydroxide solutions Ethanolic solution	At room T° (24h)	Whilton *et al.* [152]
Tetraethoxyorthosilicate (TEOS) 3-aminopropyltrimethoxysilane (APTMS) N-[3-(trimethoxysilyl)propyl]ethylenediamine (MSPEA)			Patel *et al.* [154]
13-aminopropyltrimethoxysilane (APTMS) Tetraethoxyorthosilicate (TEOS)	Magnesium nitrate hexahydrate Sodium Hydroxide Ethanolic solution	100°C 48h	Ferreira *et al.* [164]

In 1995, Fukushima and Tani[136] proposed a one-step synthesis involving a sol-gel process to obtain an organotalc. They realized an organotalc synthesis by dissolution of magnesium chloride and an organoalcoxysilane in methanol. They obtained at room temperature a material with a talc structure which contains functional moieties $–CH_2-CH_2-CH_2-O-CO-CCH_3=CH_2$. Similarly, Burkett and Whilton[163] investigated also a one-step synthesis of organotalc using series of organoalkoxysilanes (Table 1) with lamellar structures analogous to talc. In each case, the authors confirmed the layered structure of the organotalc by X-ray powder diffraction (Figure 24). The observed reflections are broader than those from the natural talc suggesting significant interlayer disorder due to the presence of the organic moieties.

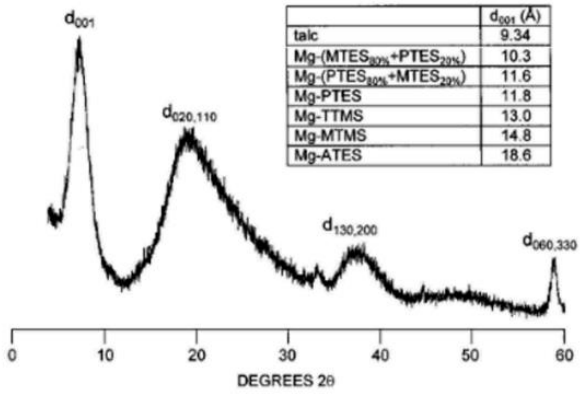

Figure 24. XRD pattern of organotalc obtained by Burkett *et al*. Reprinted with permission from ref [163].

Ukrainczyk *et al*.[137,158] evidenced the role of the length of the organic moiety in the ordering degree of talc-like hybrid: the increase of the length of organic moiety induced an increase of the ordering degree leading to a well-organized organotalc.
Fonseca *et al.*[135] were able to improve the condensation rates and the crystallinity of organotalc by realizing the sol-gel synthesis

at 100°C instead of working at room temperature. Later, Silva *et al.*[134] realized the synthesis using organoalcoxysilane (type urea) containing carbon chains with different lengths. They showed that organoalcoxysilane behaves as an anionic surfactant. Moreover, hydrophilic groups join to form micelles which facilitate the formation of covalent bond Si-O-Mg while allowing the growth of the lamellar structure.[134]

In a recent publication, Ciesielczyk *et al.*[165] confirmed the strongly influence of sol-gel process parameters on physicochemical properties of the resulting $xMgO.ySiO_2$ materials (one of these materials is similar to an organotalc). Figure 25 illustrates the three methodologies employed for the synthesis of materials via the sol-gel method. They confirmed that samples exhibiting the best morphology were obtained through simultaneous dosing of TEOS and basic catalyst into reaction system (II variant).[165]

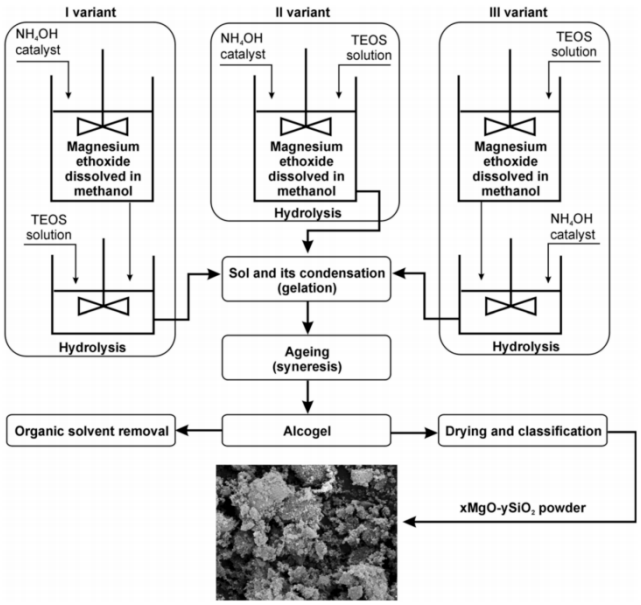

Figure 25. Methodology of precipitation of $xMgO.ySiO_2$ powders ($0.64 \leq x \leq 0.99$ and $0.83 \leq y \leq 1.00$) via the sol-gel method according to Ciesielczyk *et al.* Reprinted with permission from ref [165].

The sol-gel process allows the possibility to combine properties of organic and inorganic components. Very often the sol-gel method is exploited for the preparation of hybrid materials. In fact, this synthesis allows to obtain hybrid materials organic/inorganic with a talc matrix and with numerous functional organic moieties inserted in the interlayer space. The quality of these organotalc is considerably dependent on their purity and particle size which can be designed precisely in sol-gel process.[153,159] In view of the use of expensive chemical precursors and especially the use in excess of caustic soda, the synthesis of talc with sol-gel method is not industrially viable. Moreover, the presence of high amounts of organic compounds leads to materials having low crystallinity.

4.2. Applications of organotalc.

The hybrid materials organic/inorganic with a clay matrix are studied since around thirty years. These materials are used as environmental barriers as pollutant absorber,[166] as fillers in polymers,[167,168] as catalytic supports or as chemical sensors.[169–171] The synthesis of organotalc was motivated by various applications for which natural talc is not or is less competitive. Although the organic moieties covalently bound to the inorganic layer restrict the use of high temperature, organotalc can find a broad range of applications as detailed below.

Drug vector.

The organofunctionalities of organotalc have been investigated to improve biocompatibility of talc. For example, Yang *et al.*[170] synthesized an organotalc (3-aminopropyl functionalized talc) and incorporated a drug (flurbiprofen) into the interlayer space using different drug/clay ratios. Flurbiprofen was selected as a model drug because it is one of the widely used nonsteroidal anti-inflammatory drugs. Their results suggested that the bioavailability of flurbiprofen is improved by the use of organotalc in the drug.

Polymer nanocomposite.

The major advantage of organotalcs is its ability to be exfoliated, that is an interesting property for polymer applications. Mann *et al.*[172] showed that the delamination of organotalc could be achieved by a simple ultrasound treatment in water by creation of surface groups on lamella. Recently, Andrade *et al.*[138] reported an increase up to 54 Å of the organotalc interlayer space by functionalization of the layers with dendrimers. The growth of dendrons induced an increase of the interlamellar space and a disorganization of lamella packing. Authors highlighted the use of this dendrons-talc in a gel electrolyte for dye sensitized cells.[173] Organotalcs play also a promising role as additives in the liquid electrolyte due to the great chemical stability, exclusive swelling capacity and ion exchange potential. Moreover, Wang *et al.*[171] observed an increase of the solar cell efficiency using organotalc gel electrolyte compared to classic liquid electrolyte.

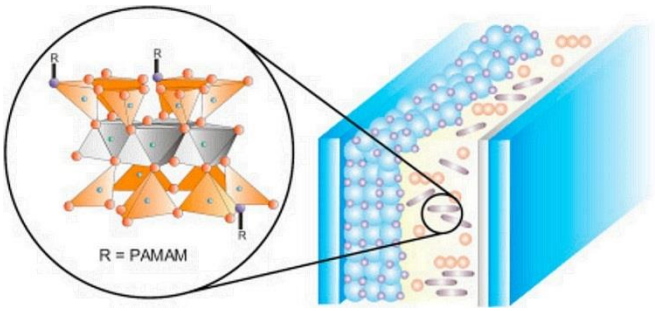

Figure 26. Scheme showing dendron-modified talcs to gel liquid electrolytes and apply to dye-sensitized solar cells. Reprinted with permission from ref [173].

Pollutant trapping.

Organotalc were also synthesized as an environmental technique solution for recovering hazardous cations. The preeminent talc features for pollutant trapping included their specific areas associated with their small particle size. However, the limitations of organotalcs as sorbents for heavy metals were their low loading capacity, small metal ion binding constants and low selectivity to diverse types of metal.[133,174] To bypass these limitations, organotalc could be functionalized with chelating functions for example. Functionalization of organotalc allowed to enhance both the heavy metal blinding capacities of organotalcs and their selectivity to specific metals. The reactivity of these organotalcs was mostly explored for cation removal, mainly those that contain nitrogen[175,176] and sulfur[177] centers attached to the pendant groups directly bonded to the inorganic matrix.[153] Organotalcs with mercapto-groups have been demonstrated to be highly efficient agents for heavy-cation removal.[178]

An organotalc containing nickel ions located in the octahedral sheet was developed by Melo *et al.*[157] for barium adsorption *via* organic chains. Dey *et al.*[179] managed to synthesize an organotalc with a silylating agent (GTPS-TU) containing both nitrogen and sulfur as metal coordination sites and explored the metal sorption affinity (Cr, Mn, Zn…).

Badshah *et al*.[133] used organotalc to investigate thermodynamics and cations sorption of pollutants contained in liquids. The organic chains of the synthetic organotalc contained several chelating sites that were used for divalent lead, copper and cadmium removal from aqueous solutions.

4.3. The grafting of organic molecules on synthetic talc.

In the second method, organo-grafted talc is obtained by formation of covalent bonds between silanols functions (located at the lateral surfaces of talc) and chemical compounds with anhydride or alkoxysilane functions.[100,106,135,180] This chemical grafting is made by condensation between the hydrolyzed organoalkoxysilane and few silanols bonds.

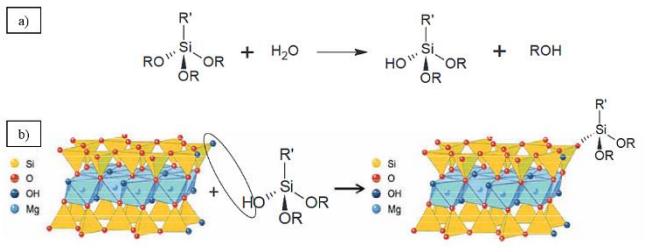

Figure 27. (a) Organoalkoxysilane hydrolysis and (b) condensation with talc. Reprinted with permission from ref [100].

Very few studies report the organoalkoxysilane grafting on talc. Da Fonseca *et al.*[181,182] highlighted the synthesis of organo-grafted natural talc (thermally activated at 473 K under vacuum for 24 hours) by using the coupling agents 3-aminopropyl-, N-propylethylenediamine and N-propyltriethylenediaminetrimethoxysilane in anhydrous conditions. Despite a chemical inertness, the authors obtained grafting rates from about 2.03 to 4.38 mmol per gram of talc according to organoalkoxysilane grafted. The synthesized materials maintain the original structure of talc (Figure 28) and organic compounds are supported on lateral surface of talc.

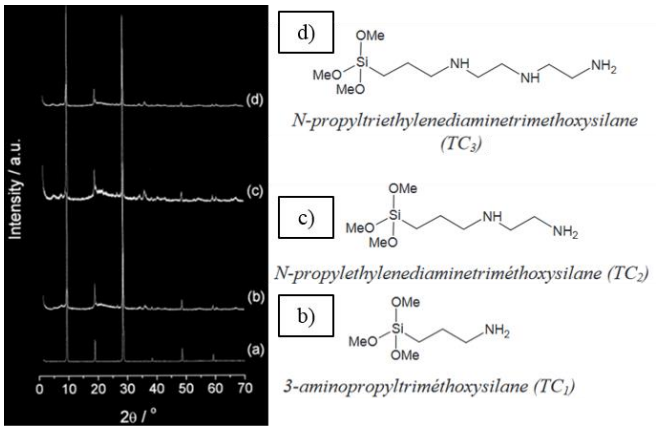

Figure 28. XRD of (a) talc and grafted talc using (b) TC_1, (c) TC_2 and d) TC_3. Reprinted with permission from ref [181].

As considered previously, Joncoux-Chabrol *et al.*[106] studied the formation of covalently linked synthetic talc (P1) with two organoalkoxysilanes (corrosion inhibitors: IM2H and HTDK, Figure 29). The influence of synthetic inorganic-organic talcs on the barrier properties of the coating deposited on carbon steel was examined. According to the authors, some properties of P1 talc-like such as the hydrophilic character, the nanoscale and the specific surface can explain the improvement of the barrier properties of the sol-gel coating.[99] Moreover, a better dispersion of the materials in the sol compared to the dispersion of natural talc was observed.

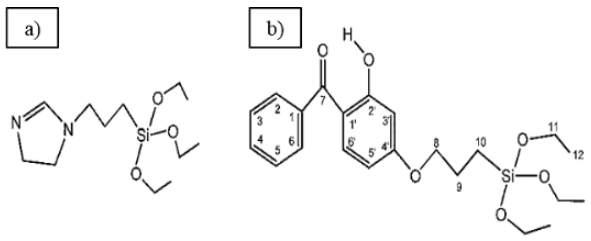

Figure 29. Structure of N-(3-triethoxysilylpropyl)-4,5-dihydroimidazole (IM2H) (a) and 2-hydroxy-4-(3-triethoxysilylpropoxy)-diphenylketone (HTDK) (b). Reprinted with permission from ref [100,106].

4.4. Hydrogel comprising an organic-talc hybrid.

Two patents describe process allowing to obtain an organic-inorganic hybrid of magnesium silicate with a talc structure, in aqueous environment, by replacing a part of the silicon precursor by an organic compound soluble in water. The principle of these processes is the same as the nanotalc synthesis (short range order and crystalline nanotalcs), i.e.:

1) Formation of an organic-talc precursor by coprecipitation reaction in aqueous medium. It is a coprecipitation between a magnesium salt, sodium metasilicate and an oxysilane soluble in water, in order to have a Si/Mg atomic ratio equal to 4/3.[183]

2) Hydrothermal treatment of this organic-talc precursor.[184] This treatment is carried out at a temperature ideally between 240°C and 250°C improving the crystallinity of the product (compared to hydrogel). This invention relates a composition comprising functionalized talc particles in which 1% to 75% of the silicon atoms are covalently bonded to organic group illustrated in Figure 30.

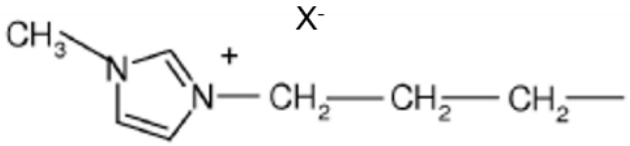

Figure 30. Chemical formula of the organic group covalently bounded to silicon atoms of the organic-inorganic hybrid talc. Reprinted with permission from ref [184].

The advantage of this process is to obtain organic-inorganic hybrid materials with important content in organic group. These inventions propose a simple and fast method compatible with industrial constraints, without production of polluting chemical compounds. Moreover, this invention is less expensive than sol-gel process since the synthesis is realized in an aqueous medium. Nevertheless, the choice of oxysilane (organic functions) is limited due to its necessary water-solubility. Compared to the grafting method, the quantity of organic function is controlled since it depends on the proportion of organic precursor used for the precipitation. These inventions also intend to offer a hydrogel that can be used as a support of ionic liquid (SIL) in catalysis.

5. Conclusions and outlook for nanotalc.

This paper offers a comprehensive review about the different natures, the synthesis methods and the applications of synthetic nanotalc. Table 2 summarizes the main features of the crystalline nanotalc, the short-range order nanotalc and the organic talc-like structure.

In the end, this review is the opportunity to redefine the main characteristics of talcous material and to distinguish natural talc mineral and synthetic talc. The term “talc” refers to the natural mineral structure with the following characteristics: i) a silicon/magnesium molar ratio of 4/3, ii) a (001) ray situated around 9.3-9.4 Å which does not vary after an ethylene glycol treatment (definition of a non-swelling phyllosilicate) and iii) a (06l-33l) ray of around 1.51-1.54 Å (characteristic of a trioctahedral phyllosilicate).

This review evidences that this talc-mineral structure is an inspiring force for the development of new materials. Synthetic nanotalc is an innovative product due to its high purity, its submicronic size and its tunable hydrophilic character (leading to be the first fluid mineral). These unique characteristics account for the reason of the great research interest over the last decades. In the last decades, this synthetic talc evolved from a geological model tool to a geo-based advanced material filler. This evolution led to improvements in its synthesis techniques. Nowadays, a new process allows the crystalline nanotalc synthesis in only a few tens of second. Regarding to its applications, nanotalc was tested, in its aqueous gel or powder form, in many areas from polymer to cosmetic industries. This innovative material was approved in various specific applications as demonstrated by the numerous application patent deposits.

Nowadays, the main challenges are to delaminate the nanotalc and to scale-up the synthesis process towards industrial production. The first challenge can be enlightened by deagglomeration of the talc precursor or by intercalation of organic compounds in the interspace layer using organotalc. For the second challenge, Supercritical fluid technology appears to be one of the most promising solution.

Table 2. Conditions, properties and applications of the synthetic talc.

Synthesis method		Conditions (T°, P°, t)	Precursors	Quantity	Properties	Applications
Hydrothermal	In batch (P3)	250-350 °C 8.6 MPa Few hours to several days	$Mg(CH_3COO)_2.4H_2O$ $Na_2SiO_3.5H_2O$ CH_3COOH $NaCH_3COO.3H_2O$	Tens of grams	Submicron size High purity High crystallinity Hydrophilic Respect of principles of the green chemis-try	**P1-nanotalc:** Lubricant composite material Anti-corrosion coating Polymer nanocomposite
	Microwave radiations route	230 °C (500W) One minute to few hours				
	In continuous	400°C 25 MPa Few tens of seconds	$Mg(CH_3COO)_2.4H_2O$ $Na_2SiO_3.5H_2O$ CH_3COOH	> One gram		**P3-nanotalc:** Polymer nanocomposite Filler for safety document Filler for cosmetic application
Precipitation		20-80°C Ambient P° Few seconds	Mg salts (chloride, sulfate and nitrate) $Na_2SiO_3.5H_2O$ HCl or NaOH	Tens of grams	Amorphous in form of agglomerate High values of specif-ic area (500 $m^2.g^{-1}$)	Polymer nanocomposite Organic compounds absorption
Sol-gel		24-100°C Ambient P° 48h	Mg salts (chloride, sulfate and nitrate) Organosiloxanes NaOH Ethanoic solution	Tens of grams	Organic compounds fixed on T layers	Drug vector Polymer nanocomposite Pollutant trapping
Grafting of organic molecules on talc		24-110°C Nitrogen atmosphere 48 h	Natural or synthetic talc Organoalkoxysiloxanes			

Acknowledgements

The authors wish to acknowledge the financial support from Imerys Compagny for the PhD grant of Marie Claverie. We acknowledge the Conseil Régional de la Nouvelle-Aquitaine.

Keywords: Phyllosilicate • organotalc. • synthetic talc • nanotalc • supercritical water •

[1] J. T. Kloprogge, S. Komarneni, J. E. Amonette, *Clays Clay Miner.* **1999**, *47*, 529–554.
[2] R. T. Martin, S. W. Bailey, D. D. Eberl, D. S. Fanning, S. Guggenheim, H. Kodama, D. R. Pevear, J. Srodon, F. J. Wicks, *Clays Clay Miner.* **1991**, *39*, 333–335.
[3] D. Zhang, C.-H. Zhou, C.-X. Lin, D.-S. Tong, W.-H. Yu, *Appl. Clay Sci.* **2010**, *50*, 1–11.
[4] S. W. Bailey, *Clays Clay Miner.* **1969**, *17*, 355–371.
[5] R. J. Haüy, *Traité de minéralogie*, Bachelier Et Huzard, **1822**.
[6] G. Agricola, *De Natura Fossilium (Textbook of Mineralogy)*, Courier Corporation, **2004**.
[7] B. W. Evans, S. Guggenheim, *Rev. Mineral. Geochem.* **1988**, *19*, 225–294.
[8] M. Soriano, M. Melgosa, M. Sánchez-Marañón, G. Delgado, E. Gámiz, R. Delgado, *Color Res. Appl.* **1998**, *23*, 178–185.
[9] M. Soriano, M. Sánchez-Marañón, M. Melgosa, E. Gámiz, R. Delgado, *Color Res. Appl.* **2002**, *27*, 430–440.
[10] J. F. Robert, P. Fragnier, L. Europe, *Macromol. Symp.* **1996**, *108*, 13–18.
[11] R. Zazenski, W. H. Ashton, D. Briggs, M. Chudkowski, J. W. Kelse, L. MacEachern, E. F. McCarthy, M. A. Nordhauser, M. T. Roddy, N. M. Teetsel, *Regul. Toxicol. Pharmacol. RTP* **1995**, *21*, 218–229.
[12] F. Martin, *Habilit. À Dir. Rech. Univ. Toulouse III Paul Sabatier* **1999**.
[13] W. Tufar, *Talc*, **2000**.
[14] J. F. Alcover, R. F. G. Jr, *ResearchGate* **1986**, *21*, 159–169.
[15] R. F. Giese, *Clays Clay Miner.* **1979**, *27*, 213–223.
[16] W. F. Bleam, *Clays Clay Miner.* **1990**, 527–536.
[17] J. H. Rayner, *Clays Clay Miner.* **1973**, *21*, 103–114.
[18] K. E. Bremmell, J. Addai-Mensah, *J. Colloid Interface Sci.* **2005**, *283*, 385–391.
[19] E. M. de C. Lobato, "Determination of Surface Free Energies and Aspect Ratio of Talc," **2004**.
[20] L. Fraichard, Nanotalcs Fonctionnalisés Vers de Nouveaux Composites Conducteurs, PhD, Université de Toulouse, Université Toulouse III - Paul Sabatier, **2012**.
[21] "Imerys Talc," can be found under http://www.imerystalc.com/, **n.d.**
[22] M. Dietemann, Étude de La Précipitation Du Silicate de Magnésium Amorphe Assistée Par Ultrasons: Synthèse, Caractérisation et Modélisation, PhD, Université de Toulouse, Université Toulouse III - Paul Sabatier, **2012**.
[23] L. F. Gate, *Preparation of Aqueous Suspensions of Talc*, **1984**, US4430249 (A).
[24] A. Usuki, M. Kawasumi, Y. Kojima, A. Okada, T. Kurauchi, O. Kamigaito, *J. Mater. Res.* **1993**, *8*, 1174–1178.
[25] A. Usuki, Y. Kojima, M. Kawasumi, A. Okada, Y. Fukushima, T. Kurauchi, O. Kamigaito, *J. Mater. Res.* **1993**, *8*, 1179–1184.
[26] Y. Kojima, A. Usuki, M. Kawasumi, A. Okada, Y. Fukushima, T. Kurauchi, O. Kamigaito, *J. Mater. Res.* **1993**, *8*, 1185–1189.
[27] Y. Kojima, A. Usuki, M. Kawasumi, A. Okada, T. Kurauchi, O. Kamigaito, *J. Appl. Polym. Sci.* **1993**, *49*, 1259–1264.
[28] C. Nkoumbou, F. Villieras, O. Barres, I. Bihannic, M. Pelletier, A. Razafitianamaharavo, V. Metang, C. Yonta Ngoune, D. Njopwouo, J. Yvon, *Clay Miner.* **2008**, *43*, 317–337.
[29] C. Nkoumbou, F. Villieras, D. Njopwouo, C. Yonta Ngoune, O. Barres, M. Pelletier, A. Razafitianamaharavo, J. Yvon, *Appl. Clay Sci.* **2008**, *41*, 113–132.
[30] L. A. Castillo, S. E. Barbosa, P. Maiza, N. J. Capiati, *Part. Sci. Technol.* **2014**, *32*, 1–7.
[31] P. Bacchin, J.-P. Bonino, F. Martin, M. Combacau, P. Barthes, S. Petit, J. Ferret, *Colloids Surf. Physicochem. Eng. Asp.* **2006**, *272*, 211–219.
[32] J. Alexis, C. Gaussens, B. Etcheverry, J.-P. Bonino, *Mater. Chem. Phys.* **2013**, *137*, 723–733.
[33] R. P. Orosco, M. del C. Ruiz, L. I. Barbosa, J. A. González, *Int. J. Miner. Process.* **2011**, *101*, 116–120.
[34] G. Alfano, P. Saba, M. Surracco, *Int. J. Miner. Process.* **1996**, *44*, 327–336.
[35] L. Godet-Morand, A. Chamayou, J. Dodds, *Powder Technol.* **2002**, *128*, 306–313.
[36] L. A. Pérez-Maqueda, A. Duran, J. L. Pérez-Rodríguez, *Appl. Clay Sci.* **2005**, *28*, 245–255.
[37] S. Sakthivel, B. Pitchumani, *Part. Sci. Technol.* **2011**, *29*, 441–449.
[38] S. Sakthivel, R. Prasanna Venkatesh, *Int. J. Min. Sci. Technol.* **2012**, *22*, 651–655.
[39] W. s. DePolo, D. g. Baird, *Polym. Compos.* **2009**, *30*, 188–199.
[40] F. Martin, J.-P. Bonino, P. Bacchin, S. Vaillant, E. Ferrage, *(En) Composite Material Consisting of a Metal Matrix and Talc (Fr) Materiau Composite Constitue Par Une Matrice Metallique Et Du Talc.*, **2004**, WO 2004063428 A1-FR 2848219 B1.
[41] K. Derya, H. Ö. Toplan, *J. Ceram. Process. Res.* **2015**, *16*, 544–547.
[42] O. F. Tuttle, *Am. J. Sci.* **1948**, *246*, 628–635.
[43] R. Roy, E. F. Osborn, *Econ. Geol.* **1952**, *47*, 717–721.
[44] N. L. Bowen, O. F. Tuttle, *Geol. Soc. Am. Bull.* **1949**, *60*, 439–460.
[45] D. Roy, R. Roy, *Am. Mineral.* **1955**, *40*, 147–178.
[46] W. Johannes, *Am. J. Sci.* **1969**, *267*, 1083–1104.
[47] R. W. T. Wilkins, J. Ito, *Am. Mineral.* **1967**, *52*, 1649.
[48] G. Martin, A. Renouprez, G. Dalmai-Imelik, B. Imelik, *Comptes Rendus Acad Sci Ser II* **1970**, *161*.
[49] G. Whitney, D. Eberl, *Am. Mineral.* **1982**, *67*, 944–949.
[50] H. Mondésir, Le Système Ni-Mg-Si-H_2O Entre 25 et 250˚Degré C : Mesure Des Coefficients de Partage Solide/Solution Pour Le Couple Ni/Mg : Cristallochimie et Stabilité Des Lizardites, Talcs, Kérolites et Stevensites de Synthèse, PhD, Université de Paris-Sud - Faculté des Sciences d'Orsay, **1987**.
[51] A. Decarreau, H. Mondésir, G. Besson, *Comptes Rendus Acad Sci Ser II* **1989**, *308*, 301–306.
[52] F. Martin, S. Petit, A. Decarreau, O. Grauby, J. L. Hazemann, Y. Noack, *Thin Solid Films* **1992**, *222*, 189–195.
[53] F. Martin, P. Ildefonse, J.-L. Hazemann, S. Petit, O. Grauby, A. Decarreau, *Eur. J. Mineral.* **1996**, 289–300.
[54] F. Martin, Etude Cristallographique et Cristallochimique de l'incorporation Du Germanium et Du Gallium Dans Les Phyllosilicates : Approche Par Synthèse Minérale, PhD, Université de Droit, d'Economie et des Sciences d'Aix-Marseille, **1994**.
[55] A. Dumas, F. Martin, E. Ferrage, P. Micoud, C. Le Roux, S. Petit, *Appl. Clay Sci.* **2013**, *85*, 8–18.
[56] F. Martin, J. Ferret, C. Lebre, S. Petit, O. Grauby, J.-P. Bonino, D. Arseguel, A. Decarreau, E. Ferrage, *(en) Method for Preparing a Synthetic Talc Composition from a Kerolite Composition (fr) Procédé De Préparation D'une Composition De Talc Synthétique Á Partir D'une Composition De Kérolites*, **2008**, WO 2008009801 A2-FR 2903682 A1.
[57] C. Lèbre, Elaboration et caractérisation de talcs synthétiques pour l'amélioration des propriétés physiques des matériaux composites industriels (revêtement de surface, plastiques, peintures...), PhD thesis, Université Paul Sabatier, **2007**.
[58] D. Arseguel, J.-P. Bonino, A. Decarreau, E. Ferrage, J. Ferret, O. Grauby, C. Lebre, F. Martin, S. Petit, *(En) Method for Preparing Talcose Compositions Comprising Synthetic Mineral Particles Containing Silicon, Germanium and Metal (Fr) Procédé De Préparation De Compositions Talqueuses Comprenant Des Particules Minérales Silico/Germano-Métalliques Synthétiques*, **2008**, WO 2008009799 A1-FR 2903680 A1.
[59] C. Le Roux, F. Martin, P. Micoud, A. Dumas, *(En) Method for Preparing a Composition Including Synthetic Inorganic Particles (Fr) Procédé De Préparation D'une Composition Comprenant Des Particules Minérales Synthétiques*, **2012**, WO 2012085239 A1-FR 2969594 A1.
[60] Y. K. Kharaka, W. W. Carothers, R. J. Rosenbauer, *Geochim. Cosmochim. Acta* **1983**, *47*, 397–402.
[61] S. E. Drummond, D. A. Palmer, *Geochim. Cosmochim. Acta* **1986**, *50*, 825–833.
[62] D. A. Palmer, S. . Drummond, *Geochim. Cosmochim. Acta* **1986**, *50*, 813–823.
[63] A. Dumas, C. Le Roux, F. Martin, P. Micoud, *(En) Process for Preparing a Composition Comprising Synthetic Mineral Particles and Composition (Fr) Procédé De Préparation D'une Composition Comprenant Des Particules Minérales Synthétiques Et Composition*, **2013**, WO 2013004979 A1-FR 2977580 A1.
[64] A. Dumas, F. Martin, C. Le Roux, P. Micoud, S. Petit, E. Ferrage, J. Brendle, O. Grauby, *Phys. Chem. Miner.* **2013**, *40*, 361–373.
[65] A. Dumas, Élaboration de Nouveaux Procédés de Synthèse et Caractérisation de Talcs Sub-Microniques : De La Recherche Fondamentale Vers Des Applications Industrielles, PhD, Université de Toulouse, Université Toulouse III - Paul Sabatier, **2013**.
[66] M. Damm, T. N. Glasnov, C. O. Kappe, *Org. Process Res. Dev.* **2009**, *14*, 215–224.
[67] R. Deul, E. U. Franck, *Berichte Bunsenges. Für Phys. Chem.* **1991**, *95*, 847–853.
[68] A. Kruse, E. Dinjus, *J. Supercrit. Fluids* **2007**, *39*, 362–380.
[69] T. B. Thomason, M. Modell, *Hazard. Waste* **1984**, *1*, 453–467.

[70] A. Loppinet-Serani, C. Aymonier, F. Cansell, *J. Chem. Technol. Biotechnol.* **2010**, *85*, 583–589.
[71] C. A. Meyer, R. B. McClintock, G. J. Silvestri, R. C. Spencer, *Thermodynamic and Transport Properties of Steam*, American Society Of Mechanical Engineers, **1993**.
[72] G. N. Sapkale, S. M. Patil, U. S. Surwase, P. K. Bhatbhage, *IJCS* **2010**, *8*, 729–43.
[73] S. E. Bozbag, C. Erkey, *J. Supercrit. Fluids* **2012**, *62*, 1–31.
[74] G. Brunner, *J. Supercrit. Fluids* **2009**, *47*, 373–381.
[75] R. Nagarajan, in *Supercrit. Fluid Clean.* (Eds.: S.P. Sawan, J. McHardy), William Andrew Publishing, Westwood, NJ, **1998**, pp. 38–69.
[76] S. Marre, F. Cansell, C. Aymonier, *Nanotechnology* **2006**, *17*, 4594.
[77] S. Marre, A. Erriguible, A. Perdomo, F. Cansell, F. Marias, C. Aymonier, *J. Phys. Chem. C* **2009**, *113*, 5096–5104.
[78] O. Pascu, B. Cacciuttolo, S. Marre, M. Pucheault, C. Aymonier, *J. Supercrit. Fluids* **2015**, *105*, 84–91.
[79] M. Türk, *J. Supercrit. Fluids* **1999**, *15*, 79–89.
[80] M. Türk, R. Lietzow, *AAPS PharmSciTech* **2004**, *5*, 36–45.
[81] C. Aymonier, A. Loppinet-Serani, H. Reverón, Y. Garrabos, F. Cansell, *J. Supercrit. Fluids* **2006**, *38*, 242–251.
[82] T. Adschiri, Y. Hakuta, K. Sue, K. Arai, *J. Nanoparticle Res.* **2001**, *3*, 227–235.
[83] P. M. Gallagher, M. P. Coffey, V. J. Krukonis, N. Klasutis, in *Supercrit. Fluid Sci. Technol.*, American Chemical Society, **1989**, pp. 334–354.
[84] T. Adschiri, K. Kanazawa, K. Arai, *J. Am. Ceram. Soc.* **1992**, *75*, 1019–1022.
[85] D. W. Matson, R. D. Smith, *J. Am. Ceram. Soc.* **1989**, *72*, 871–881.
[86] F. Cansell, C. Aymonier, *J. Supercrit. Fluids* **2009**, *47*, 508–516.
[87] F. Cansell, B. Chevalier, A. Demourgues, J. Etourneau, C. Even, V. Pessey, S. Petit, A. Tressaud, F. Weill, *J. Mater. Chem.* **1999**, *9*, 67–75.
[88] H. Duan, D. Wang, Y. Li, *Chem. Soc. Rev.* **2015**, *44*, 5778–5792.
[89] G. Philippot, C. Elissalde, M. Maglione, C. Aymonier, *Adv. Powder Technol.* **2014**, *25*, 1415–1429.
[90] C. Slostowski, S. Marre, J.-M. Bassat, C. Aymonier, *J. Supercrit. Fluids* **2013**, *84*, 89–97.
[91] Y. Marcus, in *Supercrit. Water*, John Wiley & Sons, Inc., **2012**, pp. 151–182.
[92] Y. Marcus, in *Supercrit. Water*, John Wiley & Sons, Inc., **2012**, pp. 100–150.
[93] E. Kiran, P. G. Debenedetti, C. J. Peters, *Supercritical Fluids: Fundamentals and Applications*, Springer Science & Business Media, **2012**.
[94] A. A. Galkin, V. V. Lunin, *Russ. Chem. Rev.* **2005**, *74*, 21.
[95] T. Voisin, A. Erriguible, david Ballenghien, D. Mateos, A. Kunegel, F. Cansell, C. Aymonier, *J. Supercrit. Fluids* **2017**, *120*, *Part 1*, 18–31.
[96] A. Dumas, M. Claverie, C. Slostowski, G. Aubert, C. Careme, C. Le Roux, P. Micoud, F. Martin, C. Aymonier, *Angew. Chem. Int. Ed.* **2016**, *55*, 9868–9871.
[97] C. Aymonier, C. Slostowski, A. Dumas, P. Micoud, C. Le Roux, F. Martin, *(En) Process for the Continuous Preparation of Phyllomineral Synthetic Particles (Fr) Procédé De Préparation De Particules Synthétiques Phyllominérales En Contínu*, **2015**, WO 2015159006 A1-FR 3019813 A1.
[98] C. Slostowski, S. Marre, O. Babot, T. Toupance, C. Aymonier, *Langmuir* **2012**, *28*, 16656–16663.
[99] K. Joncoux-Chabrol, J.-P. Bonino, M. Gressier, M.-J. Menu, N. Pébère, *Surf. Coat. Technol.* **2012**, *206*, 2884–2891.
[100] K. Joncoux-Chabrol, Synthèse et Fonctionnalisation de Phyllosilicates de Types Talc : Applications à Des Revêtements Sol-Gel Pour La Protection Contre La Corrosion, PhD, Université de Toulouse, Université Toulouse III - Paul Sabatier, **2010**.
[101] M. Alba, A. Becerro, M. Castro, A. Perdigón, *Chem. Commun.* **2000**, *0*, 37–38.
[102] F. Martin, E. Ferrage, S. Petit, P. de Parseval, L. Delmotte, J. Ferret, D. Arseguel, S. Salvi, *Eur. J. Mineral.* **2006**, 641–651.
[103] J.-P. Bonino, P. Bacchin, F. Martin, P. Barthes, E. Ferrage, W. Vautrin, S. Vaillant, *Matériau Composite Utilisable Comme Revêtement Lubrifiant*, **2006**, FR 2848219.
[104] B. Etcheverry, Adhérence, Mécanique et Tribologie Des Revêtements Composites NiP/Talc Multifonctionnels à Empreinte Écologique Réduite, PhD, Institut national polytechnique (Toulouse), **2007**.
[105] F. Martin, V. Baylac, J.-P. Bonino, J. Ferret, C. Lebre, P. Micoud, *(En) Composite Material Consisting of a Metal Matrix in Which Synthetic Lamellar Phyllosilicated Nanoparticles Are Distributed (Fr) Matériau Composite Constitué Par Une Matrice Métallique Dans Laquelle Sont Réparties Des Nanoparticules Phyllosilicatées Lamellaires Synthétiques*, **2009**, WO 2009081046 A1-FR 2925529 A1.
[106] K. Chabrol, M. Gressier, N. Pebere, M.-J. Menu, F. Martin, J.-P. Bonino, C. Marichal, J. Brendle, *J. Mater. Chem.* **2010**, *20*, 9695.
[107] B. Fiorentino, R. Fulchiron, V. Bounor-Legaré, J.-C. Majesté, J. C. Leblond, J. Duchet-Rumeau, *Appl. Clay Sci.* **2015**, *109–110*, 107–118.
[108] M. Yousfi, S. Livi, A. Dumas, C. Le Roux, J. Crépin-Leblond, M. Greenhill-Hooper, J. Duchet-Rumeau, *J. Colloid Interface Sci.* **2013**, *403*, 29–42.
[109] M. Yousfi, S. Livi, A. Dumas, J. Crépin-Leblond, M. Greenhill-Hooper, J. Duchet-Rumeau, *RSC Adv.* **2015**, *5*, 46197–46205.
[110] Q. Beuguel, J. Ville, J. Crepin-Leblond, P. Mederic, T. Aubry, *Polymer* **2015**, *62*, 109–117.
[111] Q. Beuguel, J. Ville, J. Crepin-Leblond, P. Mederic, T. Aubry, *Appl. Clay Sci.* **2017**, *135*, 253–259.
[112] M. A. Prado, G. Dias, C. Carone, R. Ligabue, A. Dumas, C. Le Roux, P. Micoud, F. Martin, S. Einloft, *J. Appl. Polym. Sci.* **2015**, *132*, 41854–41862.
[113] L. M. dos Santos, R. Ligabue, A. Dumas, C. Le Roux, P. Micoud, J.-F. Meunier, F. Martin, S. Einloft, *Eur. Polym. J.* **2015**, *69*, 38–49.
[114] A. Dumas, F. Martin, C. Le Roux, P. Micoud, *(En) Process for Preparing a Magnetic Talcous Composition, and Magnetic Talcous Composition (Fr) Procédé De Préparation D'une Composition Talqueuse Magnétique Et Composition Talqueuse Magnétique*, **2013**, WO 2013093376 A1-FR 2984872 A1.
[115] L. Fraichard, M. Gressier, M.-J. Menu, J.-P. Bonino, F. Martin, E. Flahaut, M. Greenhill-Hooper, A. Dumas, *(En) Talc Composition (Fr) Composition De Talc*, **2014**, WO2014096203–EP 2747091 A1.
[116] P. Sarrazin, *(En) Safety Document, and Synthetic Particles (Fr) Document De Securite Et Particules Synthetiques*, **2015**, WO 2015136431-FR 3018474 A1.
[117] B. Bouarfa, V. Ferrari, F. Springinsfeld, M. Chabrillangeas, L. Sebillotte-Arnaud, R. Lorant, *(en) Hydroalcoholic or Aqueous Gel of Synthetic Phyllosilicates as a Thickening, Mattifying and/or Application Homogenising Agent (fr) Gel Aqueux Ou Hydroalcoolique De Phyllosilicates Synthetiques a Titre D'agent Viscosant, Matifiant Et/Ou Homogeneisant D'application*, **2016**, WO 2016083385-FR 3028753 & FR 3028758.
[118] R. Lorant, M. Chabrillangeas, C. Jouy, M.-L. Chiron, *(en) Cosmetic Composition Comprising a Synthetic Phyllosilicate and a Polyol and/or a Uv Filter (fr) Composition Cosmetique Comprenant Un Phyllosilicate Synthetique Et Un Polyol Et/Ou Un Filtre Uv*, **2016**, WO 2016083404-FR 3028750 A1 & FR 3028755 A1.
[119] F. Springinsfeld, C. Jouy, M. Chabrillangeas, L. Arnaud-Sebillotte, R. Lorant, N. Jager Lezer, *(en) Cosmetic Composition Comprising a Synthetic Phyllosilicate and an Electrolyte and/or a Polyelectrolyte (fr) Composition Cosmetique Comprenant Un Phyllosilicate Synthetique Et Un Electrolyte Et/Ou Un Polyelectrolyte*, **2016**, WO 2016083418 A1-FR 3028756 A1 & FR 3028757.
[120] G. Kergosien, C. Li, *Compositions Filmogenes Comprenant Du Phyllosilicate Synthétique*, **2016**, FR 3028752.
[121] F. Springinsfeld, L. Arnaud-Sebillotte, V. Lechaux-Tarbouriech, *(en) Pickering-Type Emulsion Comprising a Synthetic Phyllosilicate (fr) Emulsion De Type Pickering Comprenant Un Phyllosilicate Synthetique*, **2016**, WO 2016083389 A1-FR 3028754 A1.
[122] L. Arnaud-Sebillotte, R. Lorant, M. Chabrillangeas, C. Moussay, *(en) Synthetic Phyllosilicate in Powder Form as a Mattifying and/or Application Homogenising Agent (fr) Phyllosilicate Synthetique Sous Forme De Poudre a Titre D'agent Matifiant Et/Ou Homogeneisant D'application*, **2016**, WO 2016083387-FR3028751.
[123] A. Krysztafkiewicz, L. K. Lipska, F. Ciesielczyk, T. Jesionowski, *Adv. Powder Technol.* **2004**, *15*, 549–565.
[124] F. Ciesielczyk, A. Krysztafkiewicz, T. Jesionowski, *Physicochem. Probl. Miner. Process.* **2004**, *38*, 197.
[125] F. Ciesielczyk, A. Krysztafkiewicz, T. Jesionowski, *J. Mater. Sci.* **2007**, *42*, 3831–3840.
[126] F. Ciesielczyk, A. Krysztafkiewicz, T. Jesionowski, *Physicochem. Probl. Miner. Process.* **2005**, *Vol. 39*, 155–164.
[127] M. Dietemann, F. Baillon, F. Espitalier, R. Calvet, P. Accart, S. D. Confetto, M. Greenhill-Hooper, *Chem. Eng. J.* **2013**, *215–216*, 658–670.
[128] A. Dumas, M. Mizrahi, F. Martin, F. G. Requejo, *Cryst. Growth Des.* **2015**, *15*, 5451–5463.
[129] D. R. M. Brew, F. P. Glasser, *Cem. Concr. Res.* **2005**, *35*, 85–98.
[130] F. Ciesielczyk, A. Krysztafkiewicz, K. Bula, T. Jesionowski, *Compos. Interfaces* **2010**, *17*, 481–494.
[131] F. Ciesielczyk, A. Krysztafkiewicz, T. Jesionowski, *Physicochem. Probl. Miner. Process.* **2007**, *41*, 185–193.
[132] F. Ciesielczyk, A. Krysztafkiewicz, T. Jesionowski, *Appl. Surf. Sci.* **2007**, *253*, 8435–8442.
[133] S. Badshah, C. Airoldi, *Chem. Eng. J.* **2011**, *166*, 420–427.
[134] C. R. Silva, M. G. Fonseca, J. S. Barone, C. Airoldi, *Chem. Mater.* **2002**, *14*, 175–179.
[135] M. G. da Fonseca, J. S. Barone, C. Airoldi, *Clays Clay Miner.* **2000**, *48*, 638–647.
[136] Y. Fukushima, M. Tani, *J. Chem. Soc. Chem. Commun.* **1995**, 241–242.

[137] J.-C. Gallégo, M. Jaber, J. Miehé-Brendlé, C. Marichal, *New J. Chem.* **2008**, *32*, 407–412.
[138] M. A. S. Andrade, H. O. Pastore, *ACS Appl. Mater. Interfaces* **2016**, *8*, 1884–1892.
[139] C. J. Brinker, G. W. Scherer, in *Sol-Gel Sci.*, Academic Press, San Diego, **1990**, p. xvi-18.
[140] K. Kamitani, M. Uo, H. Inoue, A. Makishima, *J. Sol-Gel Sci. Technol.* **1993**, *1*, 85–92.
[141] I. Kimura, Y. Taguchi, M. Tanaka, *J. Mater. Sci.* **1999**, *34*, 1471–1475.
[142] null Tamon, null Kitamura, null Okazaki, *J. Colloid Interface Sci.* **1998**, *197*, 353–359.
[143] Ebelmen, *Recherches sur les combinaisons des acides borique et silicique avec les éthers*, Paris, France, **1846**.
[144] T. Graham, *J. Chem. Soc.* **1864**, *17*, 318–327.
[145] L. L. Hench, J. K. West, *Chem. Rev.* **1990**, *90*, 33–72.
[146] P. de Parseval, Etude minéralogique et géochimique du gisement de talc et chlorite de Trimouns (Pyrénées, France), PhD, Université de Toulouse III, **1992**.
[147] P. de Parseval, S. Y. Jiang, F. Fontan, R. C. Wang, F. Martin, J. Freeet, *ResearchGate* **2004**, *20*, 877–886.
[148] U. Schärer, P. de Parseval, M. Polvé, M. de Saint Blanquat, *Terra Nova* **1999**, *11*, 30–37.
[149] M. Nocun, R. Gajerski, S. Siwulski, *Opt. Appl.* **n.d.**, *35*, 901–906.
[150] K. A. Carrado, L. Xu, R. Csencsits, J. V. Muntean, *Chem. Mater.* **2001**, *13*, 3766–3773.
[151] K. Okamoto, M. P. Kapoor, S. Inagaki, *Chem. Commun.* **2005**, 1423–1425.
[152] N. T. Whilton, S. L. Burkett, S. Mann, *J. Mater. Chem.* **1998**, *8*, 1927–1932.
[153] J. A. A. Sales, G. C. Petrucelli, F. J. V. E. Oliveira, C. Airoldi, *J. Colloid Interface Sci.* **2006**, *297*, 95–103.
[154] H. A. Patel, S. K. Sharma, R. V. Jasra, *J. Mol. Catal. Chem.* **2008**, *286*, 31–40.
[155] Y.-C. Lee, Y.-S. Choi, M. Choi, H. Yang, K. Liu, H.-J. Shin, *Appl. Clay Sci.* **2013**.
[156] M. Jaber, J. Miehé-Brendlé, M. Roux, J. Dentzer, R. Le Dred, J.-L. Guth, *New J. Chem.* **2002**, *26*, 1597–1600.
[157] M. A. Melo Jr., F. J. V. E. Oliveira, C. Airoldi, *Appl. Clay Sci.* **2008**, *42*, 130–136.
[158] L. Ukrainczyk, R. A. Bellman, A. B. Anderson, *J. Phys. Chem. B* **1997**, *101*, 531–539.
[159] M. Jaber, J. Miéhé-Brendlé, L. Delmotte, R. Le Dred, *Microporous Mesoporous Mater.* **2003**, *65*, 155–163.
[160] M. Jaber, J. Miéhé-Brendlé, L. Delmotte, R. Le Dred, *Solid State Sci.* **2005**, *7*, 610–615.
[161] M. Richard-Plouet, S. Vilminot, M. Guillot, *New J. Chem.* **2004**, *28*, 1073.
[162] G. Kumaraswamy, Y. Deshmukh, V. V. Agrawal, P. Rajmohanan, *J. Phys. Chem. B* **2005**, *109*, 16034–16039.
[163] S. L. Burkett, A. Press, S. Mann, *Chem. Mater.* **1997**, *9*, 1071–1073.
[164] R. B. Ferreira, C. R. da Silva, H. O. Pastore, *Langmuir* **2008**, *24*, 14215–14221.
[165] F. Ciesielczyk, M. Przybysz, J. Zdarta, A. Piasecki, D. Paukszta, T. Jesionowski, *J. Sol-Gel Sci. Technol.* **2014**, *71*, 501–513.
[166] C. Y. Liao, J. Y. Chiou, J. J. Lin, *RSC Adv.* **2015**, *5*, 100702–100708.
[167] M. Arroyo, M. A. López-Manchado, B. Herrero, *Polymer* **2003**, *44*, 2447–2453.
[168] M. U. Wahit, A. Hassan, Z. A. Mohd Ishak, A. R. Rahmat, N. Othman, *Polym. J.* **2006**, *38*, 767–780.
[169] Z. Yan, C. Wang, L. Hou, J. Liu, S. Jiang, Q. Liu, *Food Anal. Methods* **2016**, DOI 10.1007/s12161-016-0614-3.
[170] L. Yang, S.-K. Choi, H.-J. Shin, H.-K. Han, *Int. J. Nanomedicine* **2013**, *8*, 4147–4155.
[171] X. Wang, S. A. Kulkarni, B. I. Ito, S. K. Batabyal, K. Nonomura, C. C. Wong, M. Grätzel, S. G. Mhaisalkar, S. Uchida, *ACS Appl. Mater. Interfaces* **2013**, *5*, 444–450.
[172] S. Mann, S. L. Burkett, S. A. Davis, C. E. Fowler, N. H. Mendelson, S. D. Sims, D. Walsh, N. T. Whilton, *Chem. Mater.* **1997**, *9*, 2300–2310.
[173] M. A. S. Andrade Jr., A. F. Nogueira, K. Miettunen, A. Tiihonen, P. D. Lund, H. O. Pastore, *J. Power Sources* **2016**, *325*, 161–170.
[174] L. Mercier, C. Detellier, *Environ. Sci. Technol.* **1995**, *29*, 1318–1323.
[175] M. G. da Fonseca, C. Airoldi, *J. Mater. Chem.* **2000**, *10*, 1457–1463.
[176] M. G. da Fonseca, E. C. da Silva Filho, R. S. A. Machado Junior, L. N. H. Arakaki, J. G. P. Espinola, C. Airoldi, *J. Solid State Chem.* **2004**, *177*, 2316–2322.
[177] M. G. da Fonseca, C. Airoldi, *Thermochim. Acta* **2000**, *359*, 1–9.
[178] I. L. Lagadic, M. K. Mitchell, B. D. Payne, *Environ. Sci. Technol.* **2001**, *35*, 984–990.
[179] R. K. Dey, A. S. Oliveira, T. Patnaik, V. K. Singh, D. Tiwary, C. Airoldi, *J. Solid State Chem.* **2009**, *182*, 2010–2017.
[180] J. M. Raquez, Y. Nabar, R. Narayan, P. Dubois, *Macromol. Mater. Eng.* **2008**, *293*, 310–320.
[181] M. G. da Fonseca, C. Airoldi, *Mater. Res. Bull.* **2001**, *36*, 277–287.
[182] M. G. da Fonseca, C. Airoldi, *J. Therm. Anal. Calorim.* **2001**, *64*, 273–280.
[183] A. Dumas, C. Le Roux, F. Martin, P. Micoud, *(En) Method for Preparing a Hydrogel Comprising Silico-Metallic Mineral Particles and Hydrogel (Fr) Procédé De Préparation D'un Hydrogel Comprenant Des Particules Minérales Silico-Métalliques Et Hydrogel*, **2013**, WO 2013093339 A1-FR2984869 A1.
[184] A. Dumas, C. Le Roux, F. Martin, P. Micoud, E. Gardes, *(En) Method for Preparing a Composition Comprising Functionalised Silico/Germano-Metal Particles and Composition Obtained (Fr) Procédé De Préparation D'une Composition Comprenant Des Particules Silico/Germano-Métalliques Fonctionnalisées Et Composition Obtenue*, **2014**, WO 2014202920 A1-FR 3007405 A1.

The growing interest in synthetic talc, for polymer reinforcement and new cosmetic formulations, has motivated research to propose novel synthesis routes based on the chemistry of materials. In this context, over the past 30 years, the synthesis process of talc has evolved noticeably leading to processes which could fulfill industrial requirements. In this review, the different natures, the synthesis methods and the applications of synthetic nanotalc are enlightened with a focus on the crystalline nanotalc.

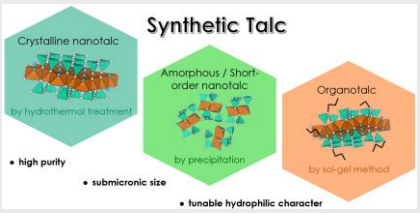

Marie Claverie, Angela Dumas, Christel Careme, Mathilde Poirier, Christophe Le Roux, Pierre Micoud, François Martin, and Cyril Aymonier.

Page No. – Page No.

Synthetic talc and talc-like structures: preparation, features and applications.